Electronic Supplementary Information

Developing Sustainable, High-Performance Perovskites in Photocatalysis: Design Strategies and Applications

Haoxin Mai,[a] Dehong Chen,[*a] Yasuhiro Tachibana,[b] Hajime Suzuki,[c] Ryu Abe[c] and Rachel A. Caruso[*a]

[a]Applied Chemistry and Environmental Science, School of Science, STEM College, RMIT University, GPO Box 2476, Melbourne, Victoria 3001, Australia

E-mail: dehong.chen@rmit.edu.au; rachel.caruso@rmit.edu.au

[b]School of Engineering, STEM College, RMIT University, Bundoora, Victoria 3083, Australia

[c]Department of Energy and Hydrocarbon Chemistry, Graduate School of Engineering, Kyoto University, Katsura, Nishikyo-ku, Kyoto 615-8510, Japan

Note S1. Principles of photocatalytic water splitting

The schematic illustration of the basic principle of the water splitting reaction on a photocatalyst is presented in Figure S1a.[1-3] When the photocatalyst absorbs photons with an energy greater than the bandgap energy of the photocatalyst, electrons (e^-) move to the conduction band (CB), leaving holes (h^+, positive charge) in the valence band (VB). These electrons and holes then move through the photocatalyst to the surface. The electrons and holes can recombine during this process, or once at the surface they can initiate redox reactions provided the band energies of the photocatalyst are well matched to the reactants. For example, the electrons and holes can trigger the H^+ reduction and H_2O oxidation, respectively. For continuous water splitting, the reduction and oxidation reactions must occur simultaneously to prevent the build-up of charge. The reactions in the water splitting process are shown in Equations (S1)-(S3):

Overall water splitting: $2H_2O + h\upsilon \rightarrow 2H_2 + O_2$ (S1)

Oxygen evolution reaction (OER): $2H_2O + 4h^+ \rightarrow 4H^+ + O_2$ (S2)

Hydrogen evolution reaction (HER): $4H^+ + 4e^- \rightarrow 2H_2$ (S3)

The HER and OER take place at a standard reduction potential of H^+/H (pH = 0, vs the standard hydrogen electrode (SHE)) and O_2/H_2O (pH = 0, vs SHE) of 0 V and 1.23 V, respectively. In order to split two water molecules and generate one oxygen molecule, the change in Gibbs free energy is +4.92 eV, indicating that the overall water splitting reaction is not thermodynamically favorable.[4] To produce a single oxygen molecule requires multiple unfavorable steps, not only due to the O_2/H_2O potential but also the kinetic hindrance arising from the anodic overpotential. Therefore, the OER is usually the bottleneck in water splitting.[5, 6]

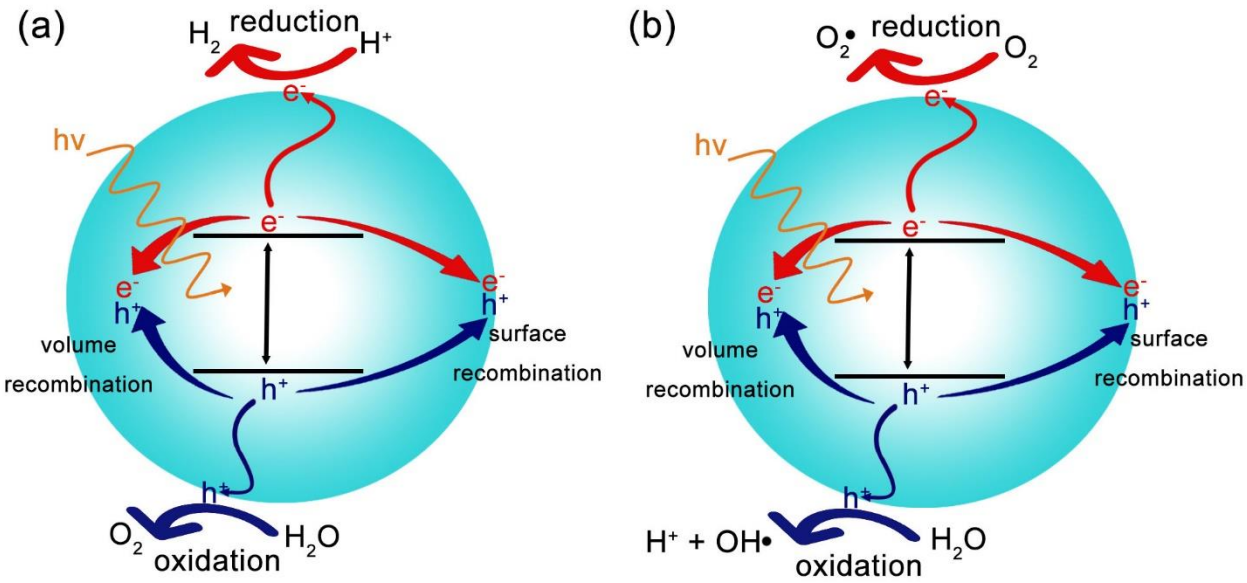

Figure S1. Illustration of the (a) overall photocatalytic water splitting reaction and (b) the production of radicals for photocatalytic pollutant degradation

In terms of the mechanism of photocatalytic water splitting, the process can be divided into three components: light absorption, charge separation and transport, and surface reaction. To maximize solar light absorbance, the bandgap of the photocatalysts should be as narrow as possible but wider than the thermodynamic requirement of 1.23 eV. However, sufficient oxidizing and reducing power from the photocatalysts must be ensured. As shown in Figure 4, the bottom of the CB (CB minima, CBM) must be more negative (lower) than the potential of H^+/H (0 V *vs.* SHE at pH = 0), while the top of the VB (VB maxima, VBM) must be more positive (higher) than the potential of O_2/H_2O (1.23 V *vs.* SHE at pH = 0) for the water splitting reaction to be facilitated. Shifting the VB position to more positive potentials or the CB position to more negative potentials would increase the oxidizing or reducing power of the photocatalysts, respectively.[7] Thus improving solar absorption by decreasing the bandgap constrains the actual photoactivity. In the context of charge separation and transport, despite the coexistence of bulk and surface recombination, surface recombination is expected to be dominant in nanometer-sized photocatalysts, as the diffusion distance to the surface is short. One method to prevent surface recombination is fast removal of one of the charge carriers. Hole scavengers, such as methanol, are often used to prevent the electron-hole recombination by hole depletion and guarantee the hydrogen production.[7, 8] Another method for reducing recombination is spatial charge separation within the material. Using this approach, one strategy is to create surface domains where one of the charge carriers will be accepted selectively, and thus one of the half reactions would be activated and restricted on these domains. Generally these domains are electron sinks, such as Pt,[9] Au,[10] NiO_x,[11] CrO_x,[12] or carbon nanotubes.[13] Alternatively, the photoanode and photocathode can be separated spatially. As the diffusion coefficients of H^+ and OH^- in solution are high, the maximum distance between the photoanode and the photocathode in water splitting can be a few centimeters, therefore the oxidation reaction and the reduction reaction can be restricted to the photoanode and photocathode, respectively.[14] This separation of the photoelectrodes not only contributes to the efficiency, but also to the safety of the reaction by avoiding the mixing of hydrogen and oxygen. In addition, the electrode separation enables use of a wider selection of materials with a narrow bandgap to be used

as photocatalysts for water splitting as long as either the energy level of the CB is more negative than the H^+/H potential or the energy level of the VB is more positive than the O_2/H_2O potential.

Note S2. Principles of photocatalytic pollutant degradation.

Photocatalytic pollutant degradation, similar to photocatalytic water splitting, is a series of photon-induced redox reactions.[15] After absorbing the photons with energy greater than the bandgap, photogenerated electrons and holes move to the surface of the photocatalysts and produce radicals that react with the organic pollutants (Figure S1b). Different from photocatalytic water splitting in which the reactants, intermediates and products are limited, the mechanism of photocatalytic degradation is complex. In simple terms, once the OH• forms, organic pollutants attached to the surface will be oxidized, and when complete degradation occurs CO_2, H_2O and ions are produced. The reactions can be represented by the following Equations:

$$OH^- + h^+ \rightarrow OH\bullet \quad \text{(S4)}$$

$$organic + OH\bullet \rightarrow H_2O + CO_2 \quad \text{(S5)}$$

The oxidation of the organic pollutants may also take place directly with the holes when they are tightly bound to the surface.

$$organic + h^+ \rightarrow H_2O + CO_2 \quad \text{(S6)}$$

In the half reduction reaction, absorbed oxygen molecules capture the electrons and form superoxide radicals.

$$O_{2(ads)} + e^- \rightarrow O_2^-\bullet \quad \text{(S7)}$$

These superoxide radicals may be further protonated and capture more electrons.

$$O_2^-\bullet + H^+ \rightarrow HOO\bullet \quad \text{(S8)}$$

$$HOO\bullet + e^- \rightarrow HO_2^- \quad \text{(S9)}$$

$$HO_2^- + H^+ \rightarrow H_2O_2 \quad \text{(S10)}$$

In contrast to water splitting, the overall photocatalytic degradation is thermodynamically favorable.[4] As it is widely accepted that OH• radicals are capable of oxidizing organic pollutants, the electron/hole recombination is the main obstacle for photocatalytic degradation.

Photocatalytic degradation, analogous to photocatalytic water splitting, consists primarily of three steps: light absorption, charge separation and transport, and surface reaction. To increase the breadth of solar energy utilized to the visible region, the photocatalyst bandgap is commonly manipulated.[15] Other than narrowing the bandgap, shifting the VB position to more positive potentials increases the oxidizing power of the photocatalysts, and thus it is beneficial for the formation of hydroxide radicals. On the other hand, shifting the CB position to more negative potentials would promote electron transfer to oxygen species, forming more superoxide radicals, which is then beneficial for some intermediate reactions of the degradation.[15] In addition to band alignment, the prevention of charge recombination at the particle surface is also pivotal for gaining high efficiency in photocatalytic degradation. Since the OH• radical is the most important product in this process, the electrons generated simultaneously must be removed promptly to prolong the life of the hydroxide radicals. In many cases, oxygen is used for this purpose.[16] The absorbed

oxygen molecules can readily capture electrons at the surface of the photocatalysts and form superoxide radicals. The removal of electrons prevents their accumulation and thus reduces the charge recombination rate. Alternatively, noble metals or carbon nanotubes have been loaded on the surface of photocatalysts as electron sinks to accept the photogenerated electrons.[17, 18]

Distinct from water splitting, however, separation of the oxidation and reduction reactions in different electrodes has little effect on the efficiency of degradation. This is because the diffusion coefficients of the superoxide radicals are much smaller than that of H^+ and OH^-.[19] A large distance between the active electrons and holes, therefore, may give rise to insufficient superoxide radicals to participate in the degradation occurring at the sites of OH• formation. Surface reactions, including the reactant adsorption, reaction at the active sites on the surface, and product desorption, are also key for photocatalytic degradation.[15] Unlike water splitting, in which only a few species participate, there are a large number of water contaminants that have completely different physical and chemical properties (e.g., charge, size, polarity, structure). Therefore, the diffusion of the contaminants from bulk to the surface of photocatalysts and the adsorption thereafter must be considered carefully. According to the previous assumption, that once the OH• radicals are generated and reach the contaminant molecules, the contaminants regardless of their types and properties will begin the degradation process, it is expected that the degradation rate will be enhanced provided that the adsorption of the contaminant molecules is in close proximity to the photocatalytic sites on which the OH• form.[20] Therefore, accessible surface area is important for photocatalytic degradation: increasing the surface area of the photocatalyst, and thus the photocatalytic sites, improves the efficiency of the degradation reactions.[4] Although many pollutants can be degraded into CO_2 and water (molecules that will have little to no affect on the photocatalyst surface), the formation of intermediates that adsorb to the surface may need to be considered in some cases.[21, 22]

Table S1. Summary of titanate perovskite photocatalysts, their CB, VB and Bandgap, and results from various photocatalytic reactions

Catalyst	Heterojunction/mechanism	Co-catalyst (wt%)	CB (V *vs.* SHE)	VB (V *vs.* SHE)	Band-gap (eV)	Incident light	Solution	Other parameters	H_2 evolution	O_2 evolution	Pollutant	Ref
STO single crystal					$\geqslant$ 3.2	UV	20 M NaOH		2.7 μmol h^{-1}			23
STO hierarchy sphere		Pt (1%)			3.2	UV	20% methanol		202.6 μmol h^{-1} g^{-1}			24
STO nanoparticles					3.2	UV	Water				RhB	25
STO nanocubes						UV	Water				RhB	26
STO nanoparticles		Pt (0.5%)			3.2	UV	50% methanol		276 μmol h^{-1} g^{-1}			27
						Vis			188 μmol h^{-1} g^{-1}			
Bulk STO		NiO (3%)	-0.6	2.7	3.3	UV	water		28 μmol h^{-1} g^{-1}			28
30 nm STO			-0.9	2.7	3.7				19.4 μmol h^{-1} g^{-1}			
6.5 nm STO			-0.8	2.7	3.6				3 μmol h^{-1} g^{-1}			
Macroporous STO		Pt (0.7%)			3.2	UV	10% methanol		3599 μmol h^{-1} g^{-1}			29
STO hollow sphere						UV	water				Cr(VI)	30
STO nanowires					3.1	UV	water				RhB, MO, reactive brilliant blue (KN-R)	31
STO nanocrystals		Pt (0.5%)			3.2	UV	20% methanol, 0.18 M KIO_3	{023}/{001}=35/65	711 μmol h^{-1} g^{-1}	300 μmol h^{-1} g^{-1}		32
6-facet STO nanocrystals		Pt (0.1%)			3.2	UV	Water	isotropic facets	787 μmol h^{-1} m^{-2}	381 μmol h^{-1} m^{-2}		33
		Pt (0.1%)-Co_3O_4 (0.01%)						isotropic facets	660 μmol h^{-1} m^{-2}	356 μmol h^{-1} m^{-2}		
18-facet STO nanocrystals		Pt (0.1%)						anisotropic facets	2083 μmol h^{-1} m^{-2}	1143 μmol h^{-1} m^{-2}		
		Pt (0.1%)-Co_3O_4 (0.01%)						anisotropic facets	4089 μmol h^{-1} m^{-2}	2095 μmol h^{-1} m^{-2}		
Bulk Mn-doped STO		Pt (0.5%)			2.7	Vis	10% methanol, 0.05M $AgNO_3$		0.67 μmol h^{-1} g^{-1}	9.0 μmol h^{-1} g^{-1}		34
Bulk Ru-doped STO		Pt (0.5%)			1.9	Vis	10% methanol, 0.05M $AgNO_3$		5.7 μmol h^{-1} g^{-1}	13 μmol h^{-1} g^{-1}		34
Bulk Rh-doped STO		Pt (0.5%)	-0.2	2.1	2.3 (steady state)	Vis	10% methanol, 0.05M $AgNO_3$		57.3 μmol h^{-1} g^{-1}			34
Bulk Ir-doped STO		Pt (0.5%)			2.3	Vis	10% methanol, 0.05M $AgNO_3$		28.7 μmol h^{-1} g^{-1}	1.3 μmol h^{-1} g^{-1}		34
Cr-doped STO nanoparticles						Vis	Water				$DeNO_x$	35
Cr-doped STO nanoparticles		Pt (1%)	-0.2	2.1	2.3	Vis	20% methanol		330 μmol h^{-1} g^{-1}			36
Bulk Al-doped STO		$RhCrO_x$ (0.1%), CoOOH				Solar	Water		5.7 μmol h^{-1} cm^{-2}	2.8 μmol h^{-1} cm^{-2}		37

		(0.3%), TiO_2 (3%)										
Fe-doped STO nanoparticles						Vis	Water				RhB	[38]
Fe-doped STO nanoshperes			-0.4	2.2	2.6	Vis	Water				Tetracy-cline (TC)	[39]
Bulk Cr,Ta-codpoed STO		Pt (1%)				Vis	6.5% methanol		70 μmol h^{-1} g^{-1}			[40]
Bulk Cr,Sb-copoded STO		Pt (0.3%)	-0.2	2.2	2.4	Vis	8% methanol		156 μmol h^{-1} g^{-1}			[41]
Bulk Ni,Ta-codoped STO		Pt (0.1%)			2.8	Vis	10% methanol, 0.02 M $AgNO_3$		8 μmol h^{-1} g^{-1}			[42]
La,Cr-codoped STO nanoparticles		Pt (0.5%)			2.1	Vis	15% methanol, 5 M NaOH		1089 μmol h^{-1} g^{-1}			[43]
Bulk Ag,Nb-codoped STO			-0.2	2.6	2.8	Vis	Water				CH_3CHO	[44]
Bulk La,Rh-codoped STO	$BiVO_4$:Mo-Au/Z-scheme	Ru/RuO_x	-0.4	2.5		Solar	Water	Reaction pressure: 10 kPa	20 μmol h^{-1} cm^{-2}	10 μmol h^{-1} cm^{-2}		[45]
Bulk La,Ni-codoped STO						Vis	Water				Malachite Green (MG)	[46]
Mesoporous N-doped STO					2.9	Vis	Water				MB,MO,RhB	[47]
F-doped STO nanoparticles					3.0	UV	gas				NO_x	[48]
Bulk La,N-codoped STO			-0.6	2.2	2.8	Vis	gas				2-propanol	[49]
Cr,N-codoped STO nanoparticles		Pt (0.5%)	-0.6	1.8	2.4	Vis	15% methanol		427 μmol h^{-1} g^{-1}			[50]
Bulk $SiTrO_{3-x}$		Pt (0.3%)				Vis	gas	CO_2/H_2O generates methane			CO_2	[51]
$SiTrO_{3-x}$ nanoparticles		Pt (1%)			3.2	UV	25% methanol, 1 M NaOH		2200 μmol h^{-1} g^{-1}			[52]
$SiTrO_{3-x}$ nanoparticles			-0.39	2.8	3.2	Solar	10% methanol, 0.05 M $AgNO_3$	Density of oxygen vacancy: 6.7 × 10^{19}	10 μmol h^{-1} g^{-1}	18 μmol h^{-1} g^{-1}		[53]
STO nanoparticles		Ni/NiO_x (2.3%)				Solar	Water		6 μmol h^{-1} g^{-1}	3 μmol h^{-1} g^{-1}		[54]
Cr-doped STO nanoparticles	Ag_3PO_4 / Type II		-0.45	2.05	2.5	Vis	Gas	Ag_3PO_4 / Cr-STO = 1:4			CO_2	[55]
STO nanoparticles	Ag_3PO_4 / Type II		-0.79 / 0.25	2.45 / 2.67	3.24 / 2.42	Vis	0.02 M $AgNO_3$	Ag_3PO_4 / STO = 1:20		1316 μmol h^{-1} g^{-1}		[56]
STO nanocubes	BiOBr / Type II		-0.71 / 0.22	2.51 / 3.12	3.22 / 2.90	Vis	Water	BiOBr / STO = 9:1			Reactive blue 198, Reactive black 5, Reactive yellow 145	[57]

STO-TiO_2 hollow multishell spheres	TiO_2 / Type II	Pt (1%)			3.2~3.3	UV	Water	3 shells	212 μmol h^{-1} g^{-1}	102 μmol h^{-1} g^{-1}		58
Bulk La,Rh-codoped STO	Ta_3N_5-Ir / Z-scheme	Ru (0.2%)				Solar	H_2SO_4, pH = 3.9		280 μmol h^{-1} g^{-1}			59
Bulk La,Cr-codoped STO	WO_3 / Z-scheme	Pt (0.5%)	-1.4	0.82	2.52	Vis	0.002 M NaI, 1% methanol		91 μmol h^{-1} g^{-1}	24 μmol h^{-1} g^{-1}		60
Cr-doped STO nanoparticles	Ag_3PO_4-MWCNTs / Z-scheme		-0.79 / 0.33	1.69 / 2.59	2.48 / 2.26	Vis	Water	Cr-STO (7.5 w%)			MG	61
STO-TiO_2 nanotubes	Au_3Cu (0.4 %) / surface plasmon					Solar	Gas	N_2H_4 as H source	725.4 μmol h^{-1} g^{-1}		CO_2	62
STO nanoparticles	Au@CdS / surface plasmon	Pt (1%)				Vis	0.05 Na_2S, 0.1 M $NaSO_3$		1091 μmol h^{-1} g^{-1}			63
$CaTiO_3$ nanoparticles			-0.65	3.0	3.65	UV	Water				As(III)	64
Bulk Cu-doped $CaTiO_3$		NiO_x				Vis	Water		22.7 μmol h^{-1} g^{-1}			65
Cu-doped $CaTiO_3$ nanoparticles					2.2~2.7	Vis	20% methanol		146 μmol h^{-1} g^{-1}			66
Na,Eu-codoped $CaTiO_3$ nanoparticles					3.3~3.5	UV	Water				MB	67
Bulk Ag,La-codoped $CaTiO_3$		Pt (0.1%)				Vis	5% methanol		10.1 μmol h^{-1} g^{-1}			68
Bulk Rh-doped $CaTiO_3$		Pt (0.1%)				Vis	10% methanol		16.6 μmol h^{-1} g^{-1}			69
La,Cr-codoped $CaTiO_3$ hollow cubes		Pt (1%)			2.49	Vis	0.05 M Na_2SO_3		164 μmol h^{-1} g^{-1}			70
$CaTiO_3$ nanoparticles	Ag/AgCl / surface plasmon, Z-scheme		$CaTiO_3$: -0.93 AgCl: -0.06	$CaTiO_3$: 2.72 AgCl: 3.2	$CaTiO_3$: 3.65 AgCl: 3.26	Vis	Water				RhB, MO, MB	71
Fe-doped $BaTiO_3$ nanoparticles					2.2~2.4	Vis	Water				MO	72, 73
Rh-doped $BaTiO_3$ nanoparticles	WO_3 / Z-scheme	Pt (0.25%)					10% methanol, 0.01 M NaI		308 μmol h^{-1} g^{-1}			74
Cr-doped $BaTiO_3$ nanoparticles							0.1 M KOH, 0.3 M N_2H_4				Nitroben-zene (NB)	75
$BaTiO_3$ nanoparticles	$CuBi_2O_4$ / Z-scheme		0.08 /-0.63	3.38 / 1.13	3.3 / 1.76	Vis	Water				Norfloxacin	76
La_2FeTiO_6 nanoparticles						UV	Water				Phenol	77
$CaCu_3Ti_4O_{12}$ nanoparticles			-0.13	2.35	2.48	Vis	Water	Octahedron shaped particles prepared in molten KCl			TC	78
$CaCu_3Ti_4O_{12}$ nanoparticles						Vis	Water	Intrinsic type II heterojunction between {001} and {111}			TC	79

Bulk $K_2La_2Ti_3O_{10}$		NiO_x (3%)			UV	0.1 M KOH		444 μmol h^{-1} g^{-1}	221 μmol h^{-1} g^{-1}		[80]
Bulk $Rb_2La_2Ti_3O_{10}$		NiO_x (4%)			UV	0.1 M RbOH		869 μmol h^{-1} g^{-1}	430 μmol h^{-1} g^{-1}		[80]
Bulk $Cs_2La_2Ti_3O_{10}$		NiO_x (3%)			UV	pH = 10		700 μmol h^{-1} g^{-1}	340 μmol h^{-1} g^{-1}		[80]
Bulk $K_2La_2Ti_3O_{10}$		Ni (3%) - Cr (0.5%)			3.63	UV	10% methanol		885 μmol h^{-1} g^{-1}	442 μmol h^{-1} g^{-1}		[81]
Zn,N-codoped $K_2La_2Ti_3O_{10}$ nanoparticles					2.67	Vis	Water				RhB	[82]
Bulk Ce-doped $K_2La_2Ti_3O_{10}$		Pt (2%)				UV	Water		50 μmol h^{-1} g^{-1}			[83]
Bulk V-doped $K_2La_2Ti_3O_{10}$						UV	0.056 M KI		96 μmol h^{-1} g^{-1}			[84]
Bulk N-doped $K_2La_2Ti_3O_{10}$					3.44	UV	0.1 M methanol		7.2 μmol h^{-1} g^{-1}			[85]
Bulk $K_2La_2Ti_3O_{10}$	CdS / light absorber					UV	0.1 M Na_2S		50.5 μmol h^{-1} g^{-1}			[86]
Bulk La,Fe-codoped Sr_2TiO_4					3.2	UV	0.05 M Na_2SO_3		1062 μmol h^{-1} g^{-1}			[87]
Bulk La,Cr-codoped Sr_2TiO_4		Pt (1%)				Vis	0.05 M Na_2SO_3		170 μmol h^{-1} g^{-1}			[88]
Bulk La,Rh-codoped Sr_2TiO_4		Pt (1%)	-0.69	1.74	2.43	Vis	0.05 M Na_2SO_3		400 μmol h^{-1} g^{-1}			[89]
La,Cr-codoped Sr_2TiO_4 nanoparticles	La,Cr-codoped STO / Type II	Pt (0.25%)			2.54	Vis	20% methanol		24 μmol h^{-1} g^{-1}			[90]
Bulk $Bi_4Ti_3O_{12}$		Pt (1%)			3.1	UV	5% methanol		0.6 μmol h^{-1} g^{-1}	3 μmol h^{-1} g^{-1}		[91]
Cr-doped $Bi_4Ti_3O_{12}$						Vis	5% methanol		58.1 μmol h^{-1} g^{-1}			[92]
$Bi_4Ti_3O_{12}$ nanosheets					2.9	UV	Water	{001} facets exposed			RhB	[93]
Cr-doped $Bi_4Ti_3O_{12}$ nanosheets					2.4	Vis	5% methanol	{010} facets are inactive	117 μmol h^{-1} g^{-1}			[93]
$Bi_4Ti_3O_{12}$ nanoparticles					3.2~3.3	UV	Water	Ultrasonic assistance			MO	[94]
$Bi_4Ti_3O_{12}$ nanosheets	Au nanorods / surface plasmon				2.47	Vis	Water				RhB, α-Naphthol (α-NP)	[95]
$Bi_4Ti_3O_{12}$ nanoparticles	CuS / Type II		-0.11 / 0.04	2.85 / 1.52	2.96 / 1.48	Vis	Water				2-methyl-4-chlorophenoxyacetic acid (MCPA)	[96]
$Bi_4Ti_3O_{12}$ nanoparticles	$CuFe_2O_4$ / Type II, p-n junction		-0.23 / 0.57	2.97 / 2.12	3.2 / 1.55	Vis	Water				MO	[97]
$Bi_4Ti_3O_{12}$ nanosheets	BiOI / Type II					Vis	Water	Positive polarization			RhB	[98]

$Bi_4Ti_3O_{12}$ nanoparticles	g-C_3N_4 / Type II, p-n junction		-0.05 / -1.12	2.79 / 1.56	2.84 / 2.68	Vis	Water				Acid Orange-II (AO-7)	[99]
$Bi_5FeTi_3O_{15}$ hierarchical flowers					2.08	Vis	Water				RhB	[100]
$Bi_5FeTi_3O_{15}$ nanoparticles with different morphologies			-0.47~-0.59	2.51-2.60	1.92~2.13	Vis	Water	Nanoflowers show the best photoactivity			TC	[101]
Bulk La-doped $Bi_5FeTi_3O_{15}$					2.0 – 2.7	Solar	Water				RhB	[102]
$Bi_5FeTi_3O_{15}$ nanosheets	g-C_3N_4 – Ag / Z-scheme		0.22 / -1.06	2.25 / 1.65	2.03 / 2.71	Vis	Water				TC	[103]
Cr,Nb-codped Bi_3TiNbO_9 nanoparticles		Pt (1%)			2.15	Vis	0.05 M Na_2SO_3		230 μmol h^{-1} g^{-1}			[104]
$Sr_2Ba_2Nb_2TiO_{12}$ nanoparticles					2.11	Solar	Gas	V_O serves as active sites			CO_2	[105]
Bulk $La_2Ti_2O_7$		NiO_x			3.8	UV	Water		614 μmol h^{-1} g^{-1}	304 μmol h^{-1} g^{-1}		[106]
Bulk Ca-doped $La_2Ti_2O_7$		NiO_x (1%)				UV	Water		850 μmol h^{-1} g^{-1}			[107]
Bulk Sr-doped $La_2Ti_2O_7$		NiO_x (1%)				UV	Water		1510 μmol h^{-1} g^{-1}			[107]
Bulk Ba-doped $La_2Ti_2O_7$		NiO_x (1%)				UV	Water		2010 μmol h^{-1} g^{-1}			[107]
Bulk Cr-doped $La_2Ti_2O_7$		Pt (1%)			2.2	Vis	33% methanol		15 μmol h^{-1} g^{-1}			[107]
Bulk Fe-doped $La_2Ti_2O_7$		Pt (1%)			2.6	Vis	33% methanol		10 μmol h^{-1} g^{-1}			[107]
N-doped $La_2Ti_2O_7$ nanosheets	g-C_3N_4 / Type II	Pt (2%)	-0.63 / -0.83	2.54 / 1.82	3.17 / 2.65	Vis	20% methanol		430 μmol h^{-1} g^{-1}			[108]
$La_2Ti_2O_7$ nanosheets	Bi_2WO_6 / Type II, p-n junction		-0.56 / 0.3	2.69 / 2.77	3.25 / 2.47	Vis	Water				RhB	[109]
$La_2Ti_2O_7$ nanoparticles	BiOBr / Type II, p-n junction		-0.39 / 0.25	3.33 / 3.03	3.72 / 2.78	Vis	Water				RhB	[110]
N-doped $La_2Ti_2O_7$ nanoparticles	r-GO-Au / surface plasmon	Pt (1.55%)				Vis	1M NaOH		163.4 μmol h^{-1} g^{-1}			[111]
$La_2Ti_2O_7$ nanosheets	black phosphorus – Au / surface plasmon		-0.43	2.9	3.33	Vis / NIR	20% methanol		Vis :740 μmol h^{-1} g^{-1}, NIR: 300 μmol h^{-1} g^{-1}			[112]
$La_2Ti_2O_7$ nanoparticles	r-GO –NiFe / hole capturer		-0.59	2.58	3.2	Solar	10% TEOA, 0.01 M $NaIO_3$		532 μmol h^{-1} g^{-1}			[113]
Bulk $La_4Ti_3O_{12}$		NiO_x (0.6%)			3.95	UV	Water		714 μmol h^{-1} g^{-1}	358 μmol h^{-1} g^{-1}		[114]
Bulk $CaLa_4Ti_4O_{15}$		NiO_x (0.2%)			3.79	UV	Water		1186 μmol h^{-1} g^{-1}	552 μmol h^{-1} g^{-1}		[114]
Bulk $SrLa_4Ti_4O_{15}$		NiO_x (0.7%)			3.82	UV	Water		2342 μmol h^{-1} g^{-1}	1092 μmol h^{-1} g^{-1}		[114]

Bulk $BaLa_4Ti_4O_{15}$	NiO_x (0.5%)		3.85	UV	Water		4600 μmol h^{-1} g^{-1}	2308 μmol h^{-1} g^{-1}		[114]
Bulk $BaLa_4Ti_4O_{15}$	Ni (0.5%)			UV	0.01 M H_3BO_3, 0.01M Na_2SO_3		480 μmol h^{-1} g^{-1}	1100 μmol h^{-1} g^{-1}	NO_3^-	[115]
Bulk $BaLa_4Ti_4O_{15}$	Ag (1%)		3.9	UV	Gas	CO_2 flow rate: 15 mL min^{-1}	67 μmol h^{-1} g^{-1}	37 μmol h^{-1} g^{-1}	CO_2	[116]
Bulk $BaLa_4Ti_4O_{15}$	$Au@Cr_2O_3$ (0.1%@0.5%)			UV	10% methanol		6064 μmol h^{-1} g^{-1}	3000 μmol h^{-1} g^{-1}		[117]

Table S2. Summary of ferrite perovskite photocatalysts, their CB, VB and Bandgap, and results from various photocatalytic reactions

Catalyst	Heterojunction/mechanism	Co-catalyst (wt%)	CB (V *vs.* SHE)	VB (V *vs.* SHE)	Bandgap (eV)	Incident light	Solution	Other parameters	H_2 evolution	O_2 evolution	Pollutant	Ref
BFO nanoparticles					1.8 – 2.3	Vis	Water	Bandgap is affected by morphologies			CR	[118]
BFO nanoparticles	Graphene				1.87	Vis	Water	Fe-O-C bonds affects bandgap			CR	[119]
BFO hollow sphere					2.1	Vis	Water				RhB, 4-Chlorophenol (4-CP)	[120]
Ba-doped BFO nanofibers						Vis	Water				CR	[119]
Ca-doped BFO nanofibers						Vis	Water				CR	[121]
Mn-doped BFO nanoparticles					1.97	Vis	Water				Acid red-58 (AR-58)	[122]
Gd-doped BFO nanoparticles					2.03	Vis	Water				RhB	[123]
Gd,Sn-codoped BFO nanoparticles					2.06	Vis	Water				CR, MB	[124]
Sr,Co-codoped BFO nanoparticles			0.445	2.315	1.87	Vis	Water				RhB	[125]
La,Se-codoped BFO nanoparticles					1.94	Vis	Water				CR	[124]
Gd,Co-codoped BFO nanoparticles					1.77	Vis	Water		74.57 μmol h^{-1} cm^{-2}			[126]
BFO-STO solid solution		Pt (1%)			2.2	Vis	0.05 M Na_2S	Sr:Bi = 0.6:0.4	50 μmol h^{-1} g^{-1}			[127]
BFO nanofibers	TiO_2 / Type II, p-n junction		0.54 / -0.3	2.63 / 2.9	2.09 / 3.2	Vis	Water				MB	[128]

BFO nanotubes array	TiO_2 / Type II, p-n junction				2.12 / 3.16	Vis	Water			RhB	[129]
Porous BFO nanoparticles	TiO_2 / Type II, p-n junction	Pt (1%)	0.21 / -0.2	2.28 / 3.0	2.07 / 3.2	Vis	20% methanol		8 μmol h^{-1} g^{-1}		[130]
BFO@TiO_2 core@shell						Vis	Water	Ultrasonic assistance		Methyl violet (MV)	[131]
BFO nanoparticles	$BiVO_4$ / Type II, p-n junction		0.6 / 0.5	2.6 / 2.8	2.0 / 2.3	Vis	Water			RhB	[132]
BFO nanocubes	g-C_3N_4 / Type II		0.10 / -1.13	2.3 / 1.57	2.2 / 2.7	Vis	Water			MO	[133]
BFO nanoparticles	g-C_3N_4 / Z-scheme		0.60 / -0.86	2.76 / 1.91	2.16 / 2.77	Vis	Water			RhB	[134]
BFO nanoparticles	g-C_3N_4 / Z-scheme		0.32 / -1.15	2.60 / 1.65	2.32 / 2.80	Vis	Water		23.31 μmol h^{-1} g^{-1}		[135]
BFO nanowires	Au / surface plasmon				2.35	Vis	4 mM $FeCl_3$			120 μmol h^{-1} g^{-1}	[136]
BFO nanoparticles	$NaYF_4$:Yb,Er / upconversion				2.0	Vis / NIR	Water			4-CP, MO	[29]
$LaFeO_3$ nanoparticles					2.0 – 2.1	Vis	Water	Bandgap is affected by morphologies		RhB	[137]
Ca-doped $LaFeO_3$ nanoparticles						Vis	Water			4-MP	[138]
floral-like $LaFeO_3$ nanostructures					2.1	Vis	Water			RhB, MB	[139]
$PrFeO_3$ nanoparticles					2.52	Vis	Water			RhB	[140]
$YFeO_3$ nanoparticles					2.46	Vis	Water			RhB	[140]
$SrFeO_3$ nanoparticles					1.80	Vis	Water			MB	[141]
$LaFeO_3$ nanoparticles	TiO_2 / Type II		0.2 / -0.3	2.2 /2.9	2.0 / 3.2	Vis	Water			RhB	[142]
Nanocast mesoporous $LaFeO_3$						Vis	Water			2-CP	[143]
Bi-doped porous $LaFeO_3$	ZnO / Type II, p-n junction		0.2 / -0.1	2.2 / 3.1	2.0 / 3.2	Vis	Water			2,4-dichlorophenol (2,4-DCP)	[144]
Ti-doped $LaFeO_3$ nanoparticles					2.1	Vis	Water			4-CP	[145]
$LaFeO_3$ nanoparticles	g-C_3N_4 / Z-scheme	Pt (3%)	0.11 / -1.28	2.03 / 1.54	1.92 / 2.82	Vis	10% TEOA		158 μmol h^{-1} g^{-1}		[146]
$LaFeO_3$ spheres	g-C_3N_4 / Z-scheme		0.02 / -0.96	2.11 / 1.94	2.09 / 2.9	Vis	Water			Brilliant Blue (BB)	[147]
Truncated hexagonal bi-pyramidal $GeFeO_3$					2.15	Vis	Water			RhB	[148]

Table S3. Summary of niobate perovskite photocatalysts, their CB, VB and Bandgap, and results from various photocatalytic reactions

Catalyst	Heterojunction/mechanism	Co-catalyst (wt%)	CB (V *vs.* SHE)	VB (V *vs.* SHE)	Bandgap (eV)	Incident light	Solution	Other parameters	H_2 evolution	O_2 evolution	Pollutant	Ref
Orthorhombic $KNbO_3$		Pt (1.5%)			3.15	UV	25% methanol	1.0 μm cubes	333 μmol h^{-1} g^{-1}			149
Tetragonal $KNbO_3$		Pt (1.5%)			3.08	UV	25% methanol	3.3 μm cubes	118 μmol h^{-1} g^{-1}			149
Cubic $KNbO_3$		Pt (1.5%)			3.24	UV	25% methanol	0.3 μm cubes	1242 μmol h^{-1} g^{-1}			149
Orthorhombic $KNbO_3$ nanowire					3.25	UV	Water	{010} {101} exposed facets			RhB	150
Monoclinic $KNbO_3$ nanowire					3.15	UV	Water	{010} {001} {100} exposed facets			RhB	150
$KNbO_3$ nanowire	Au (4.2 & 8.0 %) / surface plasmon				3.81	UV / Vis	Water	5 or 10 nm Au			RhB	151
$KNbO_3$ nanorod	Au (4.2 & 8.0 %) / surface plasmon				3.74	UV / Vis	Water	5 or 10 nm Au			RhB	151
$KNbO_3$					3.06	Solar			5 μmol h^{-1} g^{-1}			152
C-doped $KNbO_3$		Pt (0.37%)				Solar	20% methanol	Glucose as carbon precursor	211 μmol h^{-1} g^{-1}			152
C-doped $KNbO_3$		Pt (0.37%)				Vis	20% methanol	Glucose as carbon precursor	12.4 μmol h^{-1} g^{-1}			152
$KNbO_3$ nanotubes	r-GO / electron acceptor				3.13	UV Vis	Water				RhB	153
$KNbO_3$ nanoscrolls	r-GO / electron acceptor				3.13	UV	20% methanol	2% rGO	250 μmol h^{-1} g^{-1}			154
$KNbO_3$ nanoparticles	g-C_3N_4 / Type II	Pt (0.5%)	-0.81 / -1.33	2.39 / 1.57	3.20 / 2.90	Vis	Gas				CO_2	155
$KNbO_3$ nanowires	MoS_2 / Type II				3.24 / 1.35	Solar	15% TEOA	Ultrasonic assistanc	96 μmol h^{-1} g^{-1}			156
$KNbO_3$ nanoparticles	Carbon QDs / light absorber					Vis	Water		469 μmol h^{-1} g^{-1}			157
$KNbO_3$ nanorod	Ag (0.5%) / surface plasmon	Pt (0.37%)			3.13	Solar	Methanol		2116 μmol h^{-1} g^{-1}			158
$KNbO_3$ nanorod	Ag (0.1-1%) / surface plasmon				3.13	Solar	Water				RhB	158
$KNbO_3$ nanorod	Ag (0.1-1%) / surface plasmon				3.13	Solar / UV / Vis	5% ethanol				N_2 fixation	158
$KNbO_3$ nanofiber					3.63	UV-Vis	Water	Spontaneous polarization in ferroelectric $KNbO_3$			RhB	159
Cubic $NaNbO_3$		Pt (0.5%)			3.29	UV-Vis	18.5% Methanol	28.6 m^2 g^{-1}	127 μmol h^{-1} g^{-1}		CO_2 reduction	160
Orthorhombic $NaNbO_3$		Pt (0.5%)			3.45	UV-Vis	18.5% Methanol	26.4 m^2 g^{-1}	72.3 μmol h^{-1} g^{-1}		CO_2 reduction	160

$NaNbO_3$ nanofiber					3.80	UV-Vis	Water	Anti-ferroelectric		RhB	[159]
Mixed-phase $NaNbO_3$		Pt (0.5%)				UV-Vis	Gas phase	Cubic-orthorhombic surface-junctions improved charge separation		CO_2 reduction	[161]
$NaNbO_3$	g-C_3N_4 / Type II		-0.77 / -1.13	2.63 / 1.5	3.40 / 2.43	Vis	Water			CO_2 reduction	[162]
$NaNbO_3$	g-C3N4 / Type II		-0.60 / -1.08	2.81 / 1.60	3.41 / 2.68	Vis	Water	2-3 μm cubes		RhB, MO, TC	[163]
$NaNbO_3$	BiOI / p-n junction				3.40	Vis	Water			MB	[164]
$NaNbO_3$	MoS_2 / p-n junction		-0.23 / -0.29	3.04 / 1.8	3.27 / 2.09	Vis	Water	~100 nm cubes		RhB	[165]
$NaNbO_3$	$BiVO_4$ / p-n junction		-0.23 / 0.2	3.04 / 2.9	3.27 / 2.7	Vis	Water	~100 nm cubes		RhB	[165]
$NaNbO_3$	WO_3 / Z-scheme		-0.69 / 0.80	2.57 / 3.37	3.26 / 2.57	UV-Vis	Water			RhB, MB, $Cr_2O_7^{2-}$	[166]
N-doped $NaNbO_3$		Pt (0.5%)			3.18	Solar	20% methanol	Urea as N precursor	241 μmol h^{-1} g^{-1}		[167]
N-doped $NaNbO_3$	0.5% N-doped rGO / electron extractor	Pt (0.5%)			3.18	Solar	20% methanol	Urea as N precursor	2342 μmol h^{-1} g^{-1}		[167]
$AgNbO_3$		Pt (0.37%)	-0.34	1.99	2.33	Solar	20% methanol		1.5 μmol h^{-1} g^{-1}		[168]
$AgNbO_3$	g-C3N4 / Type II	Pt (0.37%)	-0.34 / -1.08	1.99 / 1.66	2.33 / 2.74	Solar	20% methanol		88.0 μmol h^{-1} g^{-1}		[168]
La-doped $AgNbO_3$					2.80	Vis	Gas phase			2-propanol decomposition	[169]
$AgNbO_3$ nanoparticles	Ag@AgCl / Type II, surface plasmon				2.75	Vis	Water			MB	[170]
$AgNbO_3$ nanoparticles	AgBr / Type II		-0.81 / 0.00	2.05 / 2.60	2.86 / 2.60	Vis	Water			MB	[171]
$AgNbO_3$-$NaNbO_3$ solid solution					2.39 – 3.0	Vis	Water	40% $NaNbO_3$		2-propanol (IPA)	[172]
$SrNb_2O_6$ bulk					3.89	UV	Water		3.4 μmol h^{-1} g^{-1}		[173]
$SrNb_2O_6$ bulk		NiO_x			3.89	UV	Water		13.3 μmol h^{-1} g^{-1}		[173]
$SrNb_2O_6$ bulk		Pt			3.89	UV	Water		35.0 μmol h^{-1} g^{-1}		[173]
$SrNb_2O_6$ nanotube					3.80	UV	Water		11.0 μmol h^{-1} g^{-1}		[173]
$SrNb_2O_6$ nanotube		NiO_x			3.80	UV	Water		40.0 μmol h^{-1} g^{-1}		[173]
$SrNb_2O_6$ nanotube		Pt			3.80	UV	Water		102.0 μmol h^{-1} g^{-1}		[173]
$SrNb_2O_6$ nanorod					3.86	UV-Vis	Water			CO_2 reduction	[174]
$Sr_2Nb_2O_7$ nanoflake					3.97	UV-Vis	Water			CO_2 reduction	[174]
$SrNb_2O_6$ nanorod		RuO_2 (0.5%)			3.90	UV	Water		435 μmol h^{-1} g^{-1}		[175]

$Sr_2Nb_2O_7$ ribbon	RuO_2 (0.5%)	4.00	UV	Water	1D single crystal	475 μmol h^{-1} g^{-1}		[175]
N-doped $KCa_2Nb_3O_{10}$ nanosheets	RhO_x (1%)		Vis	20% methanol (H_2), 0.1 M $AgNO_3$ (O_2)		0.4 μmol h^{-1} g^{-1}	25 μmol h^{-1} g^{-1}	[176]
N,Nb^{4+}-doped $KCa_2Nb_3O_{10}$ nanoparticles	Pt (0.5%)	2.47	Vis	20% methanol		1073 μmol h^{-1} g^{-1}		[177]
$KCa_2Nb_3O_{10}$ nanosheets	Ru (0.25%)		UV	Water	0.99 Na^+ exchange	393 μmol h^{-1} g^{-1}	187 μmol h^{-1} g^{-1}	[178]
$KCa_2Nb_3O_{10}$ nanoparticles	Rh_2O_3 (1%)		UV	10% methanol	Acid exchange	~1000 μmol h^{-1} g^{-1}		[179]
$KCa_2Nb_3O_{10}$ nanosheets	1 nm Pt (1%)		UV	0.01 M NaI		160 μmol h^{-1} g^{-1}	50 μmol h^{-1} g^{-1}	[180]
Bulk $Ba_5Nb_4O_{10}$	NiO (0.7%)	3.9	UV	Water		4732 μmol h^{-1} g^{-1}	2278 μmol h^{-1} g^{-1}	[181]

Table S4. Summary of other oxide perovskite photocatalysts, their CB, VB and Bandgap, and results from various photocatalytic reactions

Catalyst	Heterojunction/mechanism	Co-catalyst (wt%)	CB (V *vs.* SHE)	VB (V *vs.* SHE)	Bandgap (eV)	Incident light	Solution	Other parameters	H_2 evolution	O_2 evolution	Pollutant	Ref
Bulk Bi_2WO_6		Pt (1%)			2.8	Vis	5% methanol, 0.05 M $AgNO_3$		1.6 μmol h^{-1} g^{-1}	34 μmol h^{-1} g^{-1}		91
Bi_2WO_6 nanoparticles			0.25	3.15	2.9	Vis	Water				RhB	182
Bi_2WO_6 hollow tubes					2.85	Vis	Water				RhB	183
Bi_2WO_6 nanoparticles	$Bi_2Fe_4O_9$ / Z-scheme		0.525 / -0.9	3.225 / 1.19	2.7 / 2.09	Vis	Water				RhB	184
Bi_2WO_6 nanoparticles	WO_3-Ag / Z-scheme, surface plasmon		-0.66 / 0.88	2.16 / 3.41	2.82 / 2.53	Solar	Water				Chlorobenzene	185
Bi_2WO_6 nanoplates			0.31	2.44	2.75	Vis	Gas				CO_2	186
Bi_2WO_6 nanoplates		Co_3O_4			2.8	Solar	Water		8 μmol h^{-1} cm^{-2}			187
Flower-like Bi_2WO_6 superstructures					2.75	Vis	Water				RhB	188
Bi_2WO_6 hollow microspheres					2.76	Vis	Water	Flow rate: 0.2 mL min^{-1}			CO_2	189
Flower-like Bi_2WO_6					2.81	Vis	0.067 M alcohol				Benzylic alcohols (BA)	190
Bi_2WO_6 nanoparticles					2.94 – 3.04	Vis	Water	Bandgap is affected by morphologies			RhB	191
Bi_2WO_6 thin film deposited on stainless steel mess				3.0		Solar	Water	Thickness: 627 nm			4-CP, 4-NP	192
Bi_2WO_6 nanoplates	Hemin		0.13			Vis	Water				TC	193
Single unit cell Bi_2WO_6 layer					3.47	Solar	Gas				CO_2	194
Bi_2WO_6 2D ordered array						Vis	1 M NaOH		1.1 μmol h^{-1} cm^{-2}	0.4 μmol h^{-1} cm^{-2}		195
Gd-doped flower-like Bi_2WO_6					2.71	Vis	Water				RhB	196
Er-doped flower-like Bi_2WO_6					2.72	Vis	Water				RhB	197
Ce,F-codoped flower-like Bi_2WO_6					2.71	Vis	Water	Ce^{4+}/Ce^{3+} redox centers			RhB	198
Sm,N-codoped Bi_2WO_6 nanoplates					2.74	Vis	Water	Sm^{3+}/Sm^{2+} redox centers			RhB	199
Bi_2WO_6 nanoplates	Au / surface plasmon		-0.3	2.44	2.74	Vis	Water				BA	197
Flower-like Bi_2WO_6		Pt (0.75%)				Vis	Water				HCHO	200
Flower-like Bi_2WO_6	Ag / surface plasmon					Vis	Water				RhB, MO, MB, phenol	201

Bi_2WO_6 nanosheets	Bi / surface plaomon				~2.7	Vis	Water				BA, 1-phenylethanol	[202]
Monolayer Bi_2WO_6 nanosheets	Black phosphorus / Z-scheme	Pt (3%)	0.26 / -0.8	2.93 / 0.7	2.67 / 1.5	Vis	Water / gas		4208 μmol h^{-1} g^{-1}		NO	[203]
Bi_2WO_6 nanosheets	TiO_2 / Z-scheme		0.23 / -0.39	2.93 / 2.81	2.7 / 3.2	Vis	Water				4-NA	[10]
Bi_2WO_6 quadrilateral Nanosheets	WO_3-Cu / Z-scheme		-1.15 / -0.22	1.32 / 2.31	2.47 / 2.53	Vis	Gas				CO_2	[204]
Bi_2WO_6 nanosheets	Ti_3C_2 / electron extractor		-0.38	2.52	2.90	Solar	Water				CO_2	[205]
Bi_2WO_6 nanosheets	Amorphous BiOCl		-0.45	2.33	2.78	Vis	Toluene: acetonitrile=1:3	O_2: 1 atm			Toluene oxidation	[206]
Bulk Bi_2MoO_6					2.70	Vis	0.05 M $AgNO_3$			110 μmol h^{-1} g^{-1}		[207]
Flower-like Bi_2MoO_6	Ag_3PO_4 / Type II		-0.32 / 0.3	2.38 / 2.9	2.70 / 2.60	Vis	Water				RhB	[208]
Mesoporous Bi_2MoO_6					2.62	Vis	Water				RhB, Bisphenol A (BPA)	[209]
Bi_2MoO_6 nanowires						Vis	Water	Synthesis temperature affects morphologies			RhB, MB	[210]
Bi_2MoO_6 nanoparticles					2.58 – 2.60	Vis	Water	pH values affect morphologies			MB, MO	[211]
Bi_2MoO_6 nanosheets			-0.34	2.11	2.45	Vis	Water				BA	[212]
Bi_2MoO_6 nanosheets						Vis	Water				NB	[213]
Bi_2MoO_6 nanoparticles			-0.28 - -0.37	2.27 – 2.26	2.55 – 2.63	Vis	Water / gas	V_O affects band structure and serves as active sites			CO_2	[214]
Bi_2MoO_6 nanoparticles					2.38 – 2.52	Vis	Water	V_O affects light absorption			CIP	[214]
Hierarchical Bi_2MoO_6 spheres			-0.36 - -0.44	2.0 – 2.24	2.36 – 2.68	Vis	Water	V_O serves as electron donors			BA	[215]
Flower-like Bi_2MoO_6 spheres with oxygen vacancies	Fe_2O_3 / electron extractor		-0.53	1.81 – 1.95	2.34 – 2.48	Vis	Water				Phenol	[216]
Ce-doped Bi_2MoO_6 nanoparticles						Vis	Water				b-NNP, 4-NP, MB, RhB, MP	[217]
Zn-doped Bi_2MoO_6 nanoparticles					2.73	Vis	Water				RhB	[218]
Ti-doped Bi_2MoO_6 nanorods					2.26	Vis	Water				MB	[219]
Bi_2MoO_6 hollow spheres	AgBr-Ag / Z-scheme					Vis	Water				ARS	[220]

Bi_2MoO_6 nanosheets	AgCl-Ag / Z-scheme, surface plasmon		-0.13 / -0.06	2.45 / 3.2	2.58 / 3.26	Vis	Water				RhB, MO	[221]
Bi_2MoO_6 nanosheets	Ag_3VO_4 / Type II		-0.32 / 0.04	2.71 / 2.24	3.04 / 2.20	Vis	Water				RhB	[222]
Bi_2MoO_6 nanoparticles	Ag_3PO_4-Ag / Z-scheme		-0.31/ 0.25	2.33 / 2.67	2.64 / 2.42	Vis	Water				RhB	[223]
Bi_2MoO_6 nanoparticles	MIL(100)-Fe / Type II		-0.24 / -0.65	2.34 / 1.85	2.58 / 2.50	Vis	Water				RhB	[224]
Flower-like Bi_2MoO_6 spheres	Ag_2O / Type II, p-n junction		-0.32 / 0.14	2.32 / 1.44	2.64 / 1.30	Vis	Water				RhB	[225]
Bi_2MoO_6 nanosheets	CdS-Bi / Z-scheme	Pt (0.6%)	-0.29 / -0.52	2.33 / 1.82	2.62 / 2.34	Vis	0.25 Na_2SO_3, 0.35 Na_2S		7370 μmol h^{-1} g^{-1}			[226]
Flower-like Bi_2MoO_6 spheres	AgI / Z-scheme		-0.16 / -0.5	2.24 / 2.23	2.40 / 2.73	Vis	Water				Bacteria	[227]
Flower-like Bi_2MoO_6 spheres	Ag / surface plasmon				2.64	Vis	Water				RhB, MO, MB	[228]
Bi_2MoO_6 nanosheets	TiO_2 / Type II, Au / surface plasmon				2.75 / 3.2	Vis	Water				MB, benzene series compounds	[229]
Bi_2MoO_6 nanoparticles	Bi / Light sensitizers		-0.32	2.34	2.66	Vis	Water				RhB	[230]
Bi_2MoO_6 nanoparticles	g-C_3N_4/ Type II					Vis	Toluene	O_2 flow rate: 3 mL min^{-1}			Toluene oxidation	[231]
Bi_2MoO_6 nanoparticles	TiO_2/ Typle II				2.45/3.08	Vis	Toluene	O_2 flow rate: 3 mL min^{-1}			Toluene oxidation	[232]
Bulk $SrSnO_3$		RuO_2 (1.25%)			4.1	UV	Water		227.2 μmol h^{-1} g^{-1}	113.5 μmol h^{-1} g^{-1}		[233]
Bulk $CaSnO_3$		Pt (0.5%)	-1.46	2.98	4.44	UV	13.5% methanol		1630 μmol h^{-1} g^{-1}			[234]
$CaSnO_3$ nanocubes					4.5	UV	Water				MO	[230]
$SrSnO_3$ nanorods					4.27	UV	Water				MO	[230]
$BaSnO_3$ nanorods					3.16	UV	Water				MO	[230]
$BaSnO_3$-$SrSnO_3$ solid solution		RuO_2 (1%)			3 – 4	UV	Water	Ba:Sr = 3:1	480 μmol h^{-1} g^{-1}			[235]
$CaSnO_3$ nanocubes					4.15	UV	Water				acid blue 92, acid brown 14	[236]
$SrSnO_3$ nanorods		Pt (0.5%)			4.1	UV	15% methanol		8200 μmol h^{-1} g^{-1}			[237]
$SrSnO_3$ nanoparticles		Rh (0.025%)	-1.37	2.69	4.06	UV	10% methanol		220 μmol h^{-1} g^{-1}			[238]
$SrSnO_3$ nanoparticles		NiO_x (1%)			4.04	UV	Water		235.6 μmol h^{-1} g^{-1}			[239]
$SrSnO_3$ nanorods					3.4 – 3.6	UV	Water	{100} facets are of high activity			MB	[240]
N-doped $SrSnO_3$ nanoparticles			-0.1	2.48	2.58	Vis	Water				MB	[241]
Bulk $BaSnO_3$		Pt (0.5%)	-0.69	2.41	3.10	UV	13.5% methanol		248 μmol h^{-1} g^{-1}			[234]

Fe-doped $BaSnO_3$ nanoparticles				1.7	Vis	Water				remazol	[242]
$BaSnO_{3-x}$ nanoparticles		-0.41	1.76	2.17	Solar	Water	$NaBH_4$: 3M	127.6 μmol h^{-1} cm^{-2}	63.8 μmol h^{-1} cm^{-2}		[243]
Bulk $BaZrO_3$		-1.8	3	4.8	UV	Water		500 μmol h^{-1} g^{-1}			[244]
Sn-doped $BaZrO_3$ nanoparticles				~3.3	UV	Water		690 μmol h^{-1} g^{-1}	185 μmol h^{-1} g^{-1}		[245]
$BaZrO_3$ hollow nanoparticles		-3.29	1.75	5.04	UV	Water	With V_O	67.98 μmol h^{-1} g^{-1}			[246]
Cubic-like $BaZrO_3$ nanoparticles		-1.81	1.59	3.40	UV	10% TEOA, 0.03 M $AgNO_3$	{001} facets show high reduction ability	27.8 μmol h^{-1} g^{-1}			[247]
Bi-doped $BaZrO_3$ nanoparticles				3.35	UV	Water				MB	[248]
Fe-doped $BaZrO_3$ hollow nanoparticles		-1.63	1.21	2.84	Vis	25% methanol		9.45 μmol h^{-1} g^{-1}			[249]
Ce-doped $BaZrO_3$ hollow nanoparticles		-0.342	1.848	2.19	Vis	0.25 M Na_2SO_3, 0.35 Na_2S		823 μmol h^{-1} g^{-1}			[250]
$LaCoO_3$ hollow spheres				2.07	Vis	Water				MB	[251]
$LaCoO_3$ nanoparticles				2.32	Vis	1.5 M methanol		106 μmol h^{-1} g^{-1}			[252]
$LaNiO_3$ nanoparticles				2.42	Vis	12.5% HCHO		33 μmol h^{-1} g^{-1}			[253]
$LaNiO_3$ nanoparticles	CdS / Type II	-0.45 / -0.51	1.97 / 1.89	2.42 / 2.40	Vis	Na_2S/Na_2SO_3 0.1 M		3700 μmol h^{-1} g^{-1}			[254]
$LaNiO_3$ nanoparticles	TiO_2 / Z-scheme	-0.45 / -0.29	1.97 / 2.91	2.42 / 3.20	Vis	Water				MO	[255]
$LaMnO_3$ nanoparticles	g-C_3N_4 / Z-scheme	0.01 / -1.12	1.95 / 1.56	1.94 / 2.68	Vis	Water				TC	[256]
$LaMnO_3$ nanoparticles				1.84	Vis	Water	21 nm			RhB	[257]
$Bi_4V_2O_{11}$ nanoparticles	$BiVO_4$ / Type II			2.22 / 2.49	Vis	Water				RhB	[258]
$Bi_4V_2O_{11}$ nanoparticles	Bi_2O_3 / Type II	-0.23 / -0.93	2.61 / 1.33	2.38 / 2.26	Vis	Water				MO	[259]
$Bi_4V_2O_{11}$ nanoparticles	$ZnRh_2O_4$-Au / Z-scheme			1.65 / 1.2	Vis	Water		0.32 μmol h^{-1} g^{-1}	0.13 μmol h^{-1} g^{-1}		[260]
$Bi_4V_2O_{11}$ nanoparticles	Bi_2MoO_6 / Type II	0.46 / -0.19	2.48 / 2.43	2.02 / 2.62	Vis	Water				MB, Cr(VI)	[261]
$Bi_4V_2O_{11}$ nanoparticles	Bi_2WO_6 / Type II	0.46 / -0.26	2.61 / 3.1	2.15 / 2.84	Vis	Water				Cr(VI)	[260]
$Bi_4V_2O_{11}$ nanoparticles	CdS / Z-scheme	0.55 / -0.62	2.81 / 1.72	2.26 / 2.34	Vis	Water				CIP	[262]
$Bi_4V_2O_{11}$ nanoparticles	TiO_2 / Type II	0.61 / -0.34	2.76 / 2.95	2.15 / 3.29	Vis	Water	RhB- sensitized			RhB	[263]
$Bi_4V_2O_{11}$ nanofibers	α-phase-β-phase junction / Type II			2.16 / 2.06	Vis	Water				Cr(VI), MB, N_2 fixation	[264]

Table S5. Summary of halide perovskite-based photocatalysts, their CB, VB and Bandgap, and results from various photocatalytic reactions

Catalyst	Heterojunction/mechanism	Co-catalyst (wt%)	CB (V *vs.* SHE)	VB (V *vs.* SHE)	Bandgap (eV)	Incident light	Solution	Other parameters	H_2 evolution	O_2 evolution	Pollutant	Ref
$CsSnBr_3$ nanoparticles					1.74	Vis	Water				Violet dye	[265]
$(HDA)_2SnI_4$ nanoparticles					1.9	Vis	liquid				Indoline-2-carboxylic acids dehydrogenation	[266]
$DMASnI_3$ nanocrystals					1.32 – 2.48	Vis	Water		3.2 μmol h^{-1} g^{-1}			[267]
$MASnI_3$ nanoparticles	TiO_2 / p-n junction				1.3 / 3.2	Vis	Water				RhB	[268]
Cs_2SnI_6 nanoparticles	SnS_2 / Type II				1.32 / 2.17	Vis	50% methanol	CO_2 pressure: 1 atm			CO_2	[269]
$MA_3Bi_2I_9$ nanoparticles		Pt			1.98	Vis	Saturated HI solution		169.21 μmol h^{-1} g^{-1}			[270]
$MA_3Bi_2I_9$ nanoparticles			-1.19	1.21	2.4	Vis	Gas	Flow rate: 50 mL min^{-1}			CO_2	[271]
$Rb_3Bi_2I_9$ nanoparticles			-1.01	1.39	2.4	Vis	Gas	Flow rate: 50 mL min^{-1}			CO_2	[271]
$Cs_3Bi_2I_9$ nanoparticles			-1.27	1.23	2.5	Vis	Gas	Flow rate: 50 mL min^{-1}			CO_2	[271]
$Cs_3Bi_2I_9$ nanoparticles					1.94	Solar	Saturated HI solution with Cs_2CO_3		42 μmol h^{-1} g^{-1}			[272]
$Cs_3Bi_2I_9$ nanoparticles					1.95	Vis	Water				RhB	[273]
$Cs_3Bi_2I_9$ nanoparticles	g-C_3N_4 / z-scheme				1.8 / 2.7	Vis	Water	g-C_3N_4/$Cs_3Bi_2I_9$: 10/0.1 w%			MB, MO	[274]
$Cs_3Bi_2I_9$ nanoparticles	TiO_2 / Type II				~2.0 / 3.2	Vis	0.1 M methanol					[275]
$Cs_3Bi_2I_9$ nanoparticles	Bi_2WO_6 / z-scheme		-1.1/-0.1	0.83/2.59	1.93/2.69	Solar	Gas				CO_2: 66 μmol g^{-1} CO	[276]
$Cs_3Bi_2Br_9$ nanoparticles					2.7	Vis	Liquid				Ring-opening reactions of epoxides	[277]
$Cs_3Bi_2Br_9$ nanoparticles	SBA-15		-0.57	2.17	2.74	Vis	Liquid				Hydrocarbon oxidation	[278]
$Cs_2AgBiBr_6$ nanocubes			-0.41	2.11	2.52	Solar	Gas				CO_2	[279]
$Cs_2AgBiBr_6$ nanoparticles					2.1	Vis	Water				RhB	[280]
$Cs_2AgBiBr_6$ nanoparticles	r-GO / electron extractor					Vis	Saturated HBr and H_3PO_2 solution	2.5 w% r-GO	48.9 μmol h^{-1} g^{-1}			[281]

$Cs_2AgBiBr_6$ nanoparticles	Cu-r-GO / electron extractor		-0.6	1.4	2.0	Solar	CO_2 and H_2O vapor	10 w% Cu-r-GO			CO_2: AQY 0.89% with 93% CH_4	[282]
Cs_2AgBiI_6 ultrasmall nanoparticles			-0.93	0.89	1.82	Vis	CO_2 and H_2O vapor				CO_2: 18.9 μmol g^{-1} CO with 100% selectivity	[283]
$Cs_{2.3}MA_{0.7}Sb_2Br_9$ nanoparticles					~2.5	Vis	Liquid				Toluene, cyclohexane, 2-bromotoluene, 4-bromotoluene	[284]
$Cs_3Sb_2I_9$			~-1.2	0.82	~2.0	Vis	CO_2 and H_2O vapor				CO_2: 7.1 μmol g^{-1} CO with 100% selectivity	[285]
$Cs_3Bi_{2x}Sb_{2-2x}I_9$ nanoparticles		Pt			1.63	Solar	Saturated HI solution with Cs_2CO_3	X=0.3	926 μmol h^{-1} g^{-1}			[272]
$((CH_3)_3NH)_3Sb_2Cl_9$					3.25	UV	Water				RhB, MO	[286]

References

1 Y. Miseki, H. Kato and A. Kudo, *Energy Environ. Sci.*, 2009, **2**, 306-314.
2 X. B. Chen, S. H. Shen, L. J. Guo and S. S. Mao, *Chem. Rev.*, 2010, **110**, 6503-6570.
3 Q. Wang and K. Domen, *Chem. Rev.*, 2020, **120**, 919-985.
4 S. Pasternak and Y. Paz, *ChemPhysChem*, 2013, **14**, 2059-2070.
5 A. Valdes and G. J. Kroes, *J. Chem. Phys.*, 2009, **130**, 114701.
6 H. Dau, C. Limberg, T. Reier, M. Risch, S. Roggan and P. Strasser, *Chemcatchem*, 2010, **2**, 724-761.
7 R. M. N. Yerga, M. C. A. Galvan, F. del Valle, J. A. V. de la Mano and J. L. G. Fierro, *ChemSusChem*, 2009, **2**, 471-485.
8 Z. G. Zou, J. H. Ye, R. Abe and H. Arakawa, *Catal. Lett.*, 2000, **68**, 235-239.
9 H. Kato, M. Hori, R. Konta, Y. Shimodaira and A. Kudo, *Chem. Lett.*, 2004, **33**, 1348-1349.
10 L. Yuan, B. Weng, J. C. Colmenares, Y. G. Sun and Y. J. Xu, *Small*, 2017, **13**, 1702253.
11 K. Domen, S. Naito, T. Onishi and K. Tamaru, *J. Phys. Chem.*, 1982, **86**, 3657-3661.
12 K. Maeda, K. Teramura, D. L. Lu, N. Saito, Y. Inoue and K. Domen, *Angew. Chem., Int. Ed.*, 2006, **45**, 7806-7809.
13 A. Kongkanand, R. M. Dominguez and P. V. Kamat, *Nano Letters*, 2007, **7**, 676-680.
14 S. H. Lee and J. C. Rasaiah, *J. Chem. Phys.*, 2011, **135**, 124505.
15 M. N. Chong, B. Jin, C. W. K. Chow and C. Saint, *Water Res.*, 2010, **44**, 2997-3027.
16 H. Gerischer and A. Heller, *J. Phys. Chem.*, 1991, **95**, 5261-5267.
17 E. Grabowska, M. Marchelek, T. Klimczuk, W. Lisowski and A. Zaleska-Medynska, *J. Catal.*, 2017, **350**, 159-173.
18 S. Kedem, D. Rozen, Y. Cohen and Y. Paz, *J. Phys. Chem. C*, 2009, **113**, 14893-14899.
19 M. Okuda, T. Tsuruta and K. Katayama, *Phys. Chem. Chem. Phys.*, 2009, **11**, 2287-2292.
20 R. W. Matthews, *Water Res.*, 1986, **20**, 569-578.
21 M. I. Franch, J. Peral, X. Domenech and J. A. Ayllon, *Chem. Commun.*, 2005, DOI: 10.1039/b416598e, 1851-1853.
22 M. Nussbaum and Y. Paz, *Phys. Chem. Chem. Phys.*, 2012, **14**, 3392-3399.
23 F. T. Wagner and G. A. Somorjai, *Nature*, 1980, **285**, 559-560.
24 Y. C. Hu and L. J. Guo, *Chemcatchem*, 2015, **7**, 584-587.
25 X. Wei, G. Xu, Z. H. Ren, C. X. Xu, G. Shen and G. R. Han, *J. Am. Ceram. Soc.*, 2008, **91**, 3795-3799.
26 L. F. da Silva, W. Avansi, J. Andres, C. Ribeiro, M. L. Moreira, E. Longo and V. R. Mastelaro, *Phys. Chem. Chem. Phys.*, 2013, **15**, 12386-12393.
27 T. Puangpetch, T. Sreethawong, S. Yoshikawa and S. Chavadej, *J. Mol. Catal. A-Chem.*, 2009, **312**, 97-106.
28 T. K. Townsend, N. D. Browning and F. E. Osterloh, *ACS Nano*, 2012, **6**, 7420-7426.
29 K. Yu, C. X. Zhang, Y. Chang, Y. J. Feng, Z. Q. Yang, T. Yang, L. L. Lou and S. X. Liu, *Appl. Catal. B Environ.*, 2017, **200**, 514-520.
30 Z. K. Zheng, B. B. Huang, X. Y. Qin, X. Y. Zhang and Y. Dai, *J. Colloid Interface Sci.*, 2011, **358**, 68-72.
31 T. Y. Ma, H. Li, T. Z. Ren and Z. Y. Yuan, *RSC Adv.*, 2012, **2**, 2790-2796.
32 B. Wang, S. H. Shen and L. J. Guo, *Appl. Catal. B Environ.*, 2015, **166**, 320-326.
33 L. C. Mu, Y. Zhao, A. L. Li, S. Y. Wang, Z. L. Wang, J. X. Yang, Y. Wang, T. F. Liu, R. T. Chen, J. Zhu, F. T. Fan, R. G. Li and C. Li, *Energy Environ. Sci.*, 2016, **9**, 2463-2469.
34 R. Konta, T. Ishii, H. Kato and A. Kudo, *J. Phys. Chem. B*, 2004, **108**, 8992-8995.
35 U. Sulaeman, S. Yin and T. Sato, *Appl. Catal. B Environ.*, 2011, **105**, 206-210.
36 H. Yu, S. X. Ouyang, S. C. Yan, Z. S. Li, T. Yu and Z. G. Zou, *J. Mater. Chem.*, 2011, **21**, 11347-11351.
37 H. Lyu, T. Hisatomi, Y. Goto, M. Yoshida, T. Higashi, M. Katayama, T. Takata, T. Minegishi, H. Nishiyama, T. Yamada, Y. Sakata, K. Asakura and K. Domen, *Chem. Sci.*, 2019, **10**, 3196-3201.

38 T. H. Xie, X. Sun and J. Lin, *J. Phys. Chem. C*, 2008, **112**, 9753-9759.
39 P. Li, C. B. Liu, G. L. Wu, Y. Heng, S. Lin, A. Ren, K. H. Lv, L. S. Xiao and W. D. Shi, *RSC Adv.*, 2014, **4**, 47615-47624.
40 T. Ishii, H. Kato and A. Kudo, *J. Photochem. Photobiol. A Chem.*, 2004, **163**, 181-186.
41 H. Kato and A. Kudo, *J. Phys. Chem. B*, 2002, **106**, 5029-5034.
42 R. Niishiro, H. Kato and A. Kudo, *Phys. Chem. Chem. Phys.*, 2005, **7**, 2241-2245.
43 S. X. Ouyang, H. Tong, N. Umezawa, J. Y. Cao, P. Li, Y. P. Bi, Y. J. Zhang and J. H. Ye, *J. Am. Chem. Soc.*, 2012, **134**, 1974-1977.
44 D. F. Wang, T. Kako and J. H. Ye, *J. Am. Chem. Soc.*, 2008, **130**, 2724-2725.
45 Q. Wang, T. Hisatomi, Q. X. Jia, H. Tokudome, M. Zhong, C. Z. Wang, Z. H. Pan, T. Takata, M. Nakabayashi, N. Shibata, Y. B. Li, I. D. Sharp, A. Kudo, T. Yamada and K. Domen, *Nat. Mater.*, 2016, **15**, 611-615.
46 A. Z. Jia, X. Q. Liang, Z. Q. Su, T. Zhu and S. X. Liu, *J. Hazard. Mater.*, 2010, **178**, 233-242.
47 F. Zou, Z. Jiang, X. Q. Qin, Y. X. Zhao, L. Y. Jiang, J. F. Zhi, T. C. Xiao and P. P. Edwards, *Chem. Commun.*, 2012, **48**, 8514-8516.
48 J. S. Wang, S. Yin, Q. W. Zhang, F. Saito and T. Sato, *J. Mater. Chem.*, 2003, **13**, 2348-2352.
49 M. Miyauchi, M. Takashio and H. Tobimatsu, *Langmuir*, 2004, **20**, 232-236.
50 H. Yu, S. C. Yan, Z. S. Li, T. Yu and Z. G. Zou, *Int. J. Hydrogen Energy*, 2012, **37**, 12120-12127.
51 K. Xie, N. Umezawa, N. Zhang, P. Reunchan, Y. J. Zhang and J. H. Ye, *Energy Environ. Sci.*, 2011, **4**, 4211-4219.
52 H. Q. Tan, Z. Zhao, W. B. Zhu, E. N. Coker, B. S. Li, M. Zheng, W. X. Yu, H. Y. Fan and Z. C. Sun, *ACS Appl. Mater. Interfaces*, 2014, **6**, 19184-19190.
53 S. Nishioka, J. Hyodo, J. J. M. Vequizo, S. Yamashita, H. Kumagai, K. Kimoto, A. Yamakata, Y. Yamazaki and K. Maeda, *ACS Catal.*, 2018, **8**, 7190-7200.
54 K. Han, T. Kreuger, B. T. Mei and G. D. Mul, *ACS Catal.*, 2017, **7**, 1610-1614.
55 J. J. Guo, S. X. Ouyang, P. Li, Y. J. Zhang, T. Kako and J. H. Ye, *Appl. Catal. B Environ.*, 2013, **134**, 286-292.
56 X. J. Guan and L. J. Guo, *ACS Catal.*, 2014, **4**, 3020-3026.
57 T. Kanagaraj and S. Thiripuranthagan, *Appl. Catal. B Environ.*, 2017, **207**, 218-232.
58 Y. Z. Wei, J. Y. Wang, R. B. Yu, J. W. Wan and D. Wang, *Angew. Chem., Int. Ed.*, 2019, **58**, 1422-1426.
59 Q. Wang, T. Hisatomi, S. S. K. Ma, Y. B. Li and K. Domen, *Chem. Mater.*, 2014, **26**, 4144-4150.
60 Y. S. Jia, D. Zhao, M. R. Li, H. X. Han and C. Li, *Chinese J. Catal.*, 2018, **39**, 421-430.
61 Y. Lin, S. H. Wu, X. Li, X. Wu, C. P. Yang, G. M. Zeng, Y. R. Peng, Q. Zhou and L. Lu, *Appl. Catal. B Environ.*, 2018, **227**, 557-570.
62 Q. Kang, T. Wang, P. Li, L. Q. Liu, K. Chang, M. Li and J. H. Ye, *Angew. Chem., Int. Ed.*, 2015, **54**, 841-845.
63 S. Yu, Y. H. Kim, S. Y. Lee, H. D. Song and J. Yi, *Angew. Chem., Int. Ed.*, 2014, **53**, 11203-11207.
64 J. D. Zhuang, Q. F. Tian, S. Lin, W. B. Yang, L. H. Chen and P. Liu, *Appl. Catal. B Environ.*, 2014, **156**, 108-115.
65 H. J. Zhang, G. Chen, Y. X. Li and Y. J. Teng, *Int. J. Hydrogen Energy*, 2010, **35**, 2713-2716.
66 S. N. Lim, S. A. Song, Y.-C. Jeong, H. W. Kang, S. B. Park and K. Y. Kim, *J. Electron. Mater.*, 2017, **46**, 6096-6103.
67 M. Chen, Q. Xiong, Z. Liu, K. Qiu and X. Xiao, *Ceram. Int.*, 2020, **46**, 12111-12119.
68 J. P. Zou, L. Z. Zhang, S. L. Luo, L. H. Leng, X. B. Luo, M. J. Zhang, Y. Luo and G. C. Guo, *Int. J. Hydrogen Energy*, 2012, **37**, 17068-17077.
69 S. Nishimoto, M. Matsuda and M. Miyake, *Chem. Lett.*, 2006, **35**, 308-309.
70 R. N. Wang, S. Ni, G. Liu and X. X. Xu, *Appl. Catal. B Environ.*, 2018, **225**, 139-147.
71 Y. Wang, C. G. Niu, L. Wang, Y. Wang, X. G. Zhang and G. M. Zeng, *RSC Adv.*, 2016, **6**, 47873-47882.

72 I.C. Amaechia, A. Hadj Youssefa, G. Kolhatkara, D. Rawachb, C. Gomez-Yañezc, J.P. Claverieb, S. Suna and A. Ruedigera, *Catal. Today*, 2020, ASAP.
73 I. C. Amaechi, A. Hadj Youssef, G. Kolhatkar, D. Rawach, C. Gomez-Yañez, J. P. Claverie, S. Sun and A. Ruediger, *Catal. Today*, 2021, **360**, 90-98.
74 K. Maeda, *ACS Appl. Mater. Interfaces*, 2014, **6**, 2167-2173.
75 C. Srilakshmi, R. Saraf, V. Prashanth, G. M. Rao and C. Shivakumara, *Inorg. Chem.*, 2016, **55**, 4795-4805.
76 X. Zhang, X. Wang, J. Chai, S. Xue, R. Wang, L. Jiang, J. Wang, Z. Zhang and D. D. Dionysiou, *Appl. Catal. B Environ.*, 2020, **272**, 119017.
77 R. S. Hu, C. Li, X. Wang, Y. Sun, H. X. Jia, H. Q. Su and Y. L. Zhang, *Catal. Commun.*, 2012, **29**, 35-39.
78 R. Hailili, Z. Q. Wang, Y. X. Li, Y. H. Wang, V. K. Sharma, X. Q. Gong and C. Y. Wang, *Appl. Catal. B Environ.*, 2018, **221**, 422-432.
79 R. Hailili, Z. Q. Wang, X. Q. Gong and C. Y. Wang, *Appl. Catal. B Environ.*, 2019, **254**, 86-97.
80 T. Takata, Y. Furumi, K. Shinohara, A. Tanaka, M. Hara, J. N. Kondo and K. Domen, *Chem. Mater.*, 1997, **9**, 1063-1064.
81 C. T. K. Thaminimulla, T. Takata, M. Hara, J. N. Kondo and K. Domen, *J. Catal.*, 2000, **196**, 362-365.
82 V. Kumar, Govind and S. Uma, *J. Hazard. Mater.*, 2011, **189**, 502-508.
83 L. Liu, W. Q. Cui, Y. H. Liang and F. L. Qiu, *Acta Chim. Sin.*, 2010, **68**, 211-216.
84 Y. H. Yang, Q. Y. Chen, Z. L. Yin and J. Li, *J. Alloys Compd.*, 2009, **488**, 364-369.
85 Y. F. Huang, Y. L. Wei, S. H. Cheng, L. Q. Fan, Y. B. Li, J. M. Lin and J. H. Wu, *Sol. Energy Mater. Sol. Cells*, 2010, **94**, 761-766.
86 W. Q. Cui, L. Liu, S. S. Ma, Y. H. Liang and Z. S. Zhang, *Catal. Today*, 2013, **207**, 44-49.
87 H. Zhang, S. Ni, Y. L. Mi and X. X. Xu, *J. Catal.*, 2018, **359**, 112-121.
88 X. Q. Sun, Y. H. Xie, F. F. Wu, H. M. Chen, M. L. Lv, S. Ni, G. Liu and X. X. Xu, *Inorg. Chem.*, 2015, **54**, 7445-7453.
89 X. Q. Sun and X. X. Xu, *Appl. Catal. B Environ.*, 2017, **210**, 149-159.
90 Y. S. Jia, S. Shen, D. G. Wang, X. Wang, J. Y. Shi, F. X. Zhang, H. X. Han and C. Li, *J. Mater. Chem. A*, 2013, **1**, 7905-7912.
91 A. Kudo and S. Hijii, *Chem. Lett.*, 1999, **28**, 1103-1104.
92 H. J. Zhang, G. Chen and X. Li, *Solid State Ionics*, 2009, **180**, 1599-1603.
93 Z. W. Chen, H. Jiang, W. L. Jin and C. K. Shi, *Appl. Catal. B Environ.*, 2016, **180**, 698-706.
94 S. C. Tu, H. W. Huang, T. R. Zhang and Y. H. Zhanga, *Appl. Catal. B Environ.*, 2017, **219**, 550-562.
95 N. Li, J. J. Wu, H. B. Fang, X. H. Zhang, Y. Z. Zheng and X. Tao, *Appl. Surf. Sci.*, 2018, **448**, 41-49.
96 K. Das, D. Majhi, Y. P. Bhoi and B. G. Mishra, *Chem. Eng. J.*, 2019, **362**, 588-599.
97 W. Zhao, Y. Jin, C. H. Gao, W. Gu, Z. M. Jin, Y. L. Lei and L. S. Liao, *Mater. Chem. Phys.*, 2014, **143**, 952-962.
98 A. Al-Keisy, L. Ren, X. Xu, W. C. Hao, S. X. Dou and Y. Du, *J. Phys. Chem. C*, 2019, **123**, 517-525.
99 Y. Guo, J. H. Li, Z. Q. Gao, X. Zhu, Y. Liu, Z. B. Wei, W. Zhao and C. Sun, *Appl. Catal. B Environ.*, 2016, **192**, 57-71.
100 S. M. Sun, W. Z. Wang, H. L. Xu, L. Zhou, M. Shang and L. Zhang, *J. Phys. Chem. C*, 2008, **112**, 17835-17843.
101 R. Hailili, Z.-Q. Wang, M. Xu, Y. Wang, X.-Q. Gong, T. Xu and C. Wang, *J. Mater. Chem. A*, 2017, **5**, 21275-21290.
102 G. Naresh and T. K. Mandal, *ACS Appl. Mater. Interfaces*, 2014, **6**, 21000-21010.
103 K. Wang, J. Li and G. Zhang, *ACS Appl. Mater. Interfaces*, 2019, **11**, 27686-27696.
104 L. Jiang, S. Ni, G. Liu and X. X. Xu, *Appl. Catal. B Environ.*, 2017, **217**, 342-352.
105 H. J. Yu, J. Y. Li, Y. H. Zhang, S. Q. Yang, K. L. Han, F. Dong, T. Y. Ma and H. W. Huang, *Angew. Chem., Int. Ed.*, 2019, **58**, 3880-3884.

106 R. Abe, M. Higashi, K. Sayama, Y. Abe and H. Sugihara, *J. Phys. Chem. B*, 2006, **110**, 2219-2226.
107 D. W. Hwang, H. G. Kirn, J. S. Lee, J. Kim, W. Li and S. H. Oh, *J. Phys. Chem. B*, 2005, **109**, 2093-2102.
108 X. Y. Cai, J. Y. Zhang, M. Fujitsuka and T. Majima, *Appl. Catal. B Environ.*, 2017, **202**, 191-198.
109 J. L. Li, Y. X. Zhao, M. Y. Xia, H. An, H. C. Bai, J. J. Wei, B. L. Yang and G. D. Yang, *Appl. Catal. B Environ.*, 2020, **261**, 118244.
110 Y. H. Ao, K. D. Wang, P. F. Wang, C. Wang and J. Hou, *Appl. Catal. B Environ.*, 2016, **194**, 157-168.
111 F. K. Meng, S. K. Cushing, J. T. Li, S. M. Hao and N. Q. Wu, *ACS Catal.*, 2015, **5**, 1949-1955.
112 M. S. Zhu, X. Y. Cai, M. Fujitsuka, J. Y. Zhang and T. Majima, *Angew. Chem., Int. Ed.*, 2017, **56**, 2064-2068.
113 R. Boppella, C. H. Choi, J. Moon and D. H. Kim, *Appl. Catal. B Environ.*, 2018, **239**, 178-186.
114 A. Kudo and Y. Miseki, *Chem. Soc. Rev.*, 2009, **38**, 253-278.
115 M. Oka, Y. Miseki, K. Saito and A. Kudo, *Appl. Catal. B Environ.*, 2015, **179**, 407-411.
116 K. Iizuka, T. Wato, Y. Miseki, K. Saito and A. Kudo, *J. Am. Chem. Soc.*, 2011, **133**, 20863-20868.
117 W. Kurashige, R. Kumazawa, D. Ishii, R. Hayashi, Y. Niihori, S. Hossain, L. V. Nair, T. Takayama, A. Iwase, S. Yamazoe, T. Tsukuda, A. Kudo and Y. Negishi, *J. Phys. Chem. C*, 2018, **122**, 13669-13681.
118 S. Li, Y. H. Lin, B. P. Zhang, Y. Wang and C. W. Nan, *J. Phys. Chem. C*, 2010, **114**, 2903-2908.
119 Y. N. Feng, H. C. Wang, Y. Shen, Y. H. Lin and C. W. Nan, *Int. J. Appl. Ceram. Technol.*, 2014, **11**, 676-680.
120 Y. N. Huo, M. Miao, Y. Zhang, J. A. Zhu and H. X. Li, *Chem. Commun.*, 2011, **47**, 2089-2091.
121 Y. N. Feng, H. C. Wang, Y. D. Luo, Y. Shen and Y. H. Lin, *J. Appl. Phys.*, 2013, **113**, 146101.
122 C. Ponraj, G. Vinitha and J. Daniel, *Int. J. Green Energy*, 2019, **17**, 71-83.
123 R. Q. Guo, L. Fang, W. Dong, F. G. Zheng and M. R. Shen, *J. Phys. Chem. C*, 2010, **114**, 21390-21396.
124 S. Irfan, L. L. Li, A. S. Saleemi and C. W. Nan, *J. Mater. Chem. A*, 2017, **5**, 11143-11151.
125 A. Puhan, B. Bhushan, S. Satpathy, S. S. Meena, A. K. Nayak and D. Rout, *Appl. Surf. Sci.*, 2019, **493**, 593-604.
126 A. K. Vishwakarma, P. Tripathi, A. Srivastava, A. S. K. Sinha and O. N. Srivastava, *Int. J. Hydrogen Energy*, 2017, **42**, 22677-22686.
127 L. W. Lu, M. L. Lv, D. Wang, G. Liu and X. X. Xu, *Appl. Catal. B Environ.*, 2017, **200**, 412-419.
128 Y. C. Yang, Y. Liu, J. H. Wei, C. X. Pan, R. Xiong and J. Shi, *RSC Adv.*, 2014, **4**, 31941-31947.
129 A. S. Zhu, Q. D. Zhao, X. Y. Li and Y. Shi, *ACS Appl. Mater. Interfaces*, 2014, **6**, 671-679.
130 M. Humayun, A. Zada, Z. J. Li, M. Z. Xie, X. L. Zhang, Y. Qu, F. Raziq and L. Q. Jing, *Appl. Catal. B Environ.*, 2016, **180**, 219-226.
131 Y. L. Liu and J. M. Wu, *Nano Energy*, 2019, **56**, 74-81.
132 T. Fan, C. C. Chen and Z. H. Tang, *RSC Adv.*, 2016, **6**, 9994-10000.
133 X. F. Wang, W. W. Mao, J. Zhang, Y. M. Han, C. Y. Quan, Q. X. Zhang, T. Yang, J. P. Yang, X. A. Li and W. Huang, *J. Colloid Interface Sci.*, 2015, **448**, 17-23.
134 X. Z. Deng, C. Song, Y. L. Tong, G. L. Yuan, F. Gao, D. Q. Liu and S. T. Zhang, *Phys. Chem. Chem. Phys.*, 2018, **20**, 3648-3657.
135 H. Sepahvand and S. Sharifnia, *Int. J. Hydrogen Energy*, 2019, **44**, 23658-23668.
136 S. Li, J. M. Zhang, M. G. Kibria, Z. T. Mi, M. Chaker, D. L. Ma, R. Nechache and F. Rosei, *Chem. Commun.*, 2013, **49**, 5856-5858.
137 S. Thirumalairajan, K. Girija, N. Y. Hebalkar, D. Mangalaraj, C. Viswanathan and N. Ponpandian, *RSC Adv.*, 2013, **3**, 7549-7561.
138 F. Deganello, M. L. Tummino, C. Calabrese, M. L. Testa, P. Avetta, D. Fabbri, A. B. Prevot, E. Montoneri and G. Magnacca, *New J. Chem.*, 2015, **39**, 877-885.
139 S. Thirumalairajan, K. Girija, V. R. Mastelaro and N. Ponpandian, *New J. Chem.*, 2014, **38**, 5480-5490.

140 L. Li, M. Zhang, P. Tian, W. Gu and X. Wang, *Ceram. Int.*, 2014, **40**, 13813-13817.
141 M. Ghaffari, P. Y. Tan, M. E. Oruc, O. K. Tan, M. S. Tse and M. Shannon, *Catal. Today*, 2011, **161**, 70-77.
142 L. Q. Jing, Y. C. Qu, H. J. Su, C. H. Yao and H. G. Fu, *J. Phys. Chem. C*, 2011, **115**, 12375-12380.
143 S. Afzal, X. Quan and J. L. Zhang, *Appl. Catal. B Environ.*, 2017, **206**, 692-703.
144 M. Humayun, N. Sun, F. Raziq, X. L. Zhang, R. Yan, Z. J. Li, Y. Qu and L. Q. Jing, *Appl. Catal. B Environ.*, 2018, **231**, 23-33.
145 P. Garcia-Munoz, F. Fresno, C. Lefevre, D. Robert and N. Keller, *Appl. Catal. B Environ.*, 2020, **262**, 118310.
146 K. Xu and J. Feng, *RSC Adv.*, 2017, **7**, 45369-45376.
147 Y. Wu, H. Wang, W. Tu, Y. Liu, Y. Z. Tan, X. Z. Yuan and J. W. Chew, *J. Hazard. Mater.*, 2018, **347**, 412-422.
148 M. Mishra, I. Mukherjee, A. K. Mall, A. Mitra, S. Dash, S. Chatterjee, S. Mukherjee and A. Roy, *J. Mater. Chem. A*, 2018, **6**, 13467-13467.
149 T. T. Zhang, K. Zhao, J. G. Yu, J. Jin, Y. Qi, H. Q. Li, X. J. Hou and G. Liu, *Nanoscale*, 2013, **5**, 8375-8383.
150 T. T. Zhang, W. Y. Lei, P. Liu, J. A. Rodriguez, J. G. Yu, Y. Qi, G. Liu and M. H. Liu, *Chem. Sci.*, 2015, **6**, 4118-4123.
151 J. Y. Lan, X. M. Zhou, G. Liu, J. G. Yu, J. C. Zhang, L. J. Zhi and G. J. Nie, *Nanoscale*, 2011, **3**, 5161-5167.
152 J. X. Yu, Z. G. Chen, L. Zeng, Y. Y. Ma, Z. Feng, Y. Wu, H. J. Lin, L. H. Zhao and Y. M. He, *Sol. Energy Mater. Sol. Cells*, 2018, **179**, 45-56.
153 X. Q. Li, T. Y. Zhang, S. W. Gu, S. Z. Kang, G. D. Li and J. Mu, *Sep. Purif. Technol.*, 2013, **108**, 139-142.
154 Z. Hong, X. Q. Li, S. Z. Kang, L. X. Qin, G. D. Li and J. Mu, *Int. J. Hydrogen Energy*, 2015, **40**, 14297-14304.
155 H. F. Shi, C. L. Zhang, C. P. Zhou and G. Q. Chen, *RSC Adv.*, 2015, **5**, 93615-93622.
156 S. F. Jia, Y. P. Su, B. P. Zhang, Z. C. Zhao, S. Li, Y. F. Zhang, P. C. Li, M. Y. Xu and R. Ren, *Nanoscale*, 2019, **11**, 7690-7700.
157 Z. Qu, J. Wang, J. Tang, X. Shu, X. Liu, Z. Zhang and J. Wang, *Mol. Catal.*, 2018, **445**, 1-11.
158 P. X. Xing, S. J. Wu, Y. J. Chen, P. F. Chen, X. Hu, H. J. Lin, L. H. Zhao and Y. M. He, *ACS Sustain. Chem. Eng.*, 2019, **7**, 12408-12418.
159 Y. Huan, X. H. Wang, W. C. Hao and L. T. Li, *RSC Adv.*, 2015, **5**, 72410-72415.
160 P. Li, S. X. Ouyang, G. C. Xi, T. Kako and J. H. Ye, *J. Phys. Chem. C*, 2012, **116**, 7621-7628.
161 P. Li, H. Xu, L. Q. Liu, T. Kako, N. Umezawa, H. Abe and J. H. Ye, *J. Mater. Chem. A*, 2014, **2**, 5606-5609.
162 H. F. Shi, G. Q. Chen, C. L. Zhang and Z. G. Zou, *ACS Catal.*, 2014, **4**, 3637-3643.
163 C. J. Song, M. S. Fan, B. Hu, T. J. Chen, L. P. Wang and W. D. Shi, *CrystEngComm*, 2015, **17**, 4575-4583.
164 M. Sun, Q. Yan, Y. Shao, C. Q. Wang, T. Yan, P. G. Ji and B. Du, *Appl. Surf. Sci.*, 2017, **416**, 288-295.
165 S. Kumar, T. Malik, D. Sharma and A. K. Ganguli, *ACS Appl. Nano Mater.*, 2019, **2**, 2651-2662.
166 S. F. Chen, L. Ji, W. M. Tang and X. L. Fu, *Dalton Trans.*, 2013, **42**, 10759-10768.
167 F. L. Yang, Q. Zhang, L. Zhang, M. T. Cao, Q. Q. Liu and W. L. Dai, *Appl. Catal. B Environ.*, 2019, **257**, 117901.
168 P. F. Chen, P. X. Xing, Z. Q. Chen, X. Hu, H. J. Lin, L. H. Zhao and Y. M. He, *J. Colloid Interface Sci.*, 2019, **534**, 163-171.
169 G. Q. Li, T. Kako, D. F. Wang, Z. G. Zou and J. H. Ye, *Dalton Trans.*, 2009, DOI: 10.1039/b810126d, 2423-2427.
170 L. F. Yang, J. B. Liu, H. B. Chang and S. S. Tang, *RSC Adv.*, 2015, **5**, 59970-59975.

171 C. Wang, J. Yan, X. Y. Wu, Y. H. Song, G. B. Cai, H. Xu, J. X. Zhu and H. M. Li, *Appl. Surf. Sci.*, 2013, **273**, 159-166.
172 G. Q. Li, T. Kako, D. F. Wang, Z. G. Zou and J. Ye, *J. Solid State Chem.*, 2007, **180**, 2845-2850.
173 I. S. Cho, S. Lee, J. H. Noh, D. W. Kim, D. K. Lee, H. S. Jung, D. W. Kim and K. S. Hong, *J. Mater. Chem.*, 2010, **20**, 3979-3983.
174 R. Pang, K. Teramura, H. Asakura, S. Hosokawa and T. Tanaka, *Appl. Catal. B Environ.*, 2017, **218**, 770-778.
175 D. Chen and J. H. Ye, *Chem. Mater.*, 2009, **21**, 2327-2333.
176 S. Ida, Y. Okamoto, S. Koga, H. Hagiwara and T. Ishihara, *RSC Adv.*, 2013, **3**, 11521-11524.
177 Y. N. Zhou, T. Wen, Y. Z. Guo, B. C. Yang and Y. G. Wang, *RSC Adv.*, 2016, **6**, 64930-64936.
178 Y. Ebina, N. Sakai and T. Sasaki, *J. Phys. Chem. B*, 2005, **109**, 17212-17216.
179 H. Hata, Y. Kobayashi, V. Bojan, W. J. Youngblood and T. E. Mallouk, *Nano Letters*, 2008, **8**, 794-799.
180 T. Oshima, D. L. Lu, O. Ishitani and K. Maeda, *Angew. Chem., Int. Ed.*, 2015, **54**, 2698-2702.
181 Y. Miseki, H. Kato and A. Kudo, *Chem. Lett.*, 2006, **35**, 1052-1053.
182 T. Saison, P. Gras, N. Chemin, C. Chaneac, O. Durupthy, V. Brezova, C. Colbeau-Justin and J. P. Jolivet, *J. Phys. Chem. C*, 2013, **117**, 22656-22666.
183 S. J. Liu, Y. F. Hou, S. L. Zheng, Y. Zhang and Y. Wang, *CrystEngComm*, 2013, **15**, 4124-4130.
184 B. S. Li, C. Lai, G. M. Zeng, L. Qin, H. Yi, D. L. Huang, C. Y. Zhou, X. G. Liu, M. Cheng, P. Xu, C. Zhang, F. L. Huang and S. Y. Liu, *ACS Appl. Mater. Interfaces*, 2018, **10**, 18824-18836.
185 H. R. Zhou, Z. P. Wen, J. Liu, J. Ke, X. G. Duan and S. B. Wang, *Appl. Catal. B Environ.*, 2019, **242**, 76-84.
186 Y. Zhou, Z. P. Tian, Z. Y. Zhao, Q. Liu, J. H. Kou, X. Y. Chen, J. Gao, S. C. Yan and Z. G. Zou, *ACS Appl. Mater. Interfaces*, 2011, **3**, 3594-3601.
187 G. J. Dong, Y. J. Zhang and Y. P. Bi, *J. Mater. Chem. A*, 2017, **5**, 20594-20597.
188 L. S. Zhang, W. Z. Wang, Z. G. Chen, L. Zhou, H. L. Xu and W. Zhu, *J. Mater. Chem.*, 2007, **17**, 2526-2532.
189 H. F. Cheng, B. B. Huang, Y. Y. Liu, Z. Y. Wang, X. Y. Qin, X. Y. Zhang and Y. Dai, *Chem. Commun.*, 2012, **48**, 9729-9731.
190 Y. H. Zhang and Y. J. Xu, *RSC Adv.*, 2014, **4**, 2904-2910.
191 H. Lv, Y. M. Liu, J. Guang, Z. W. Ding and J. J. Wang, *RSC Adv.*, 2016, **6**, 80226-80233.
192 M. Zargazi and M. H. Entezari, *Appl. Catal. B Environ.*, 2019, **242**, 507-517.
193 H. Yi, M. Yan, D. L. Huang, G. M. Zeng, C. Lai, M. F. Li, X. Q. Huo, L. Qin, S. Y. Liu, X. G. Liu, B. S. Li, H. Wang, M. C. Shen, Y. K. Fu and X. Y. Guo, *Appl. Catal. B Environ.*, 2019, **250**, 52-62.
194 L. Liang, F. C. Lei, S. Gao, Y. F. Sun, X. C. Jiao, J. Wu, S. Qamar and Y. Xie, *Angew. Chem., Int. Ed.*, 2015, **54**, 13971-13974.
195 L. W. Zhang and D. Bahnemann, *ChemSusChem*, 2013, **6**, 283-290.
196 N. Tian, Y. H. Zhang, H. W. Huang, Y. He and Y. X. Guo, *J. Phys. Chem. C*, 2014, **118**, 15640-15648.
197 J. Yang, X. H. Wang, Y. M. Chen, J. Dai and S. H. Sun, *RSC Adv.*, 2015, **5**, 9771-9782.
198 H. W. Huang, K. Liu, K. Chen, Y. L. Zhang, Y. H. Zhang and S. C. Wang, *J. Phys. Chem. C*, 2014, **118**, 14379-14387.
199 F. Z. Wang, W. J. Li, S. N. Gu, H. D. Li, X. Wu and X. T. Liu, *Chem. Eur. J.*, 2016, **22**, 12859-12867.
200 D. Sun, Y. Le, C. J. Jiang and B. Cheng, *Appl. Surf. Sci.*, 2018, **441**, 429-437.
201 Q. S. Wu, Y. Cui, L. M. Yang, G. Y. Zhang and D. Z. Gao, *Sep. Purif. Technol.*, 2015, **142**, 168-175.
202 J. G. Wang, H. Liang, C. Zhang, B. Jin and Y. Men, *Appl. Catal. B Environ.*, 2019, **256**, 117874.
203 J. D. Hu, D. Y. Chen, Z. Mo, N. J. Li, Q. F. Xu, H. Li, J. H. He, H. Xu and J. M. Lu, *Angew. Chem., Int. Ed.*, 2019, **58**, 2073-2077.
204 Y. W. Teh, Y. W. Goh, X. Y. Kong, B. J. Ng, S. T. Yong and S. P. Chai, *Chemcatchem*, 2019, DOI: 10.1002/cctc.201901653, 1901653.
205 S. W. Cao, B. J. Shen, T. Tong, J. W. Fu and J. G. Yu, *Adv. Funct. Mater.*, 2018, **28**, 1800136.

206 X. Cao, Z. Chen, R. Lin, W.-C. Cheong, S. Liu, J. Zhang, Q. Peng, C. Chen, T. Han, X. Tong, Y. Wang, R. Shen, W. Zhu, D. Wang and Y. Li, *Nat. Catal.*, 2018, **1**, 704-710.
207 Y. Shimodaira, H. Kato, H. Kobayashi and A. Kudo, *J. Phys. Chem. B*, 2006, **110**, 17790-17797.
208 Y. S. Xu and W. D. Zhang, *Dalton Trans.*, 2013, **42**, 1094-1101.
209 Y. C. Hao, X. L. Dong, S. R. Zhai, X. Y. Wang, H. C. Ma and X. F. Zhang, *RSC Adv.*, 2016, **6**, 35709-35718.
210 Y. Y. Sun, W. Z. Wang, S. M. Sun and L. Zhang, *CrystEngComm*, 2013, **15**, 7959-7964.
211 D. M. Chen, Q. Hao, Z. H. Wang, H. Ding and Y. F. Zhu, *CrystEngComm*, 2016, **18**, 1976-1986.
212 K. Q. Jing, J. H. Xiong, N. Qin, Y. J. Song, L. Y. Li, Y. Yu, S. J. Liang and L. Wu, *Chem. Commun.*, 2017, **53**, 8604-8607.
213 Y. Y. Xie, X. T. Shang, D. Liu, H. B. Zhao, Y. Y. Gu, Z. Z. Zhang and X. X. Wang, *Appl. Catal. B Environ.*, 2019, **259**, 118087.
214 X. Xu, X. Ding, X. L. Yang, P. Wang, S. Li, Z. X. Lu and H. Chen, *J. Hazard. Mater.*, 2019, **364**, 691-699.
215 K. Q. Jing, W. Ma, Y. H. Ren, J. H. Xiong, B. B. Guo, Y. J. Song, S. J. Liang and L. Wu, *Appl. Catal. B Environ.*, 2019, **243**, 10-18.
216 F. Fu, H. D. Shen, X. Sun, W. W. Xue, A. Shoneye, J. N. Ma, L. Luo, D. J. Wang, J. G. Wang and J. W. Tang, *Appl. Catal. B Environ.*, 2019, **247**, 150-162.
217 Z. Dai, F. Qin, H. P. Zhao, J. Ding, Y. L. Liu and R. Chen, *ACS Catal.*, 2016, **6**, 3180-3192.
218 X. B. Zhang, L. Zhang, J. S. Hu and X. H. Huang, *RSC Adv.*, 2016, **6**, 32349-32357.
219 D. P. Dutta, A. Ballal, S. Chopade and A. Kumar, *J. Photochem. Photobiol. A Chem.*, 2017, **346**, 105-112.
220 G. H. Tian, Y. J. Chen, X. Y. Meng, J. Zhou, W. Zhou, K. Pan, C. G. Tian, Z. Y. Ren and H. G. Fu, *Chempluschem*, 2013, **78**, 117-123.
221 J. Zhang, C. G. Niu, J. Ke, L. F. Zhou and G. M. Zeng, *Catal. Commun.*, 2015, **59**, 30-34.
222 S. Jonjana, A. Phuruangrat, S. Thongtem, O. Wiranwetchayan and T. Thongtem, *Mater. Lett.*, 2016, **180**, 93-96.
223 X. Lin, J. Hou, S. S. Jiang, Z. Lin, M. Wang and G. B. Che, *RSC Adv.*, 2015, **5**, 104815-104821.
224 J. Yang, X. J. Niu, S. R. An, W. Y. Chen, J. Wang and W. Liu, *RSC Adv.*, 2017, **7**, 2943-2952.
225 J. L. Zhang, H. Liu and Z. Ma, *J. Mol. Catal. A-Chem.*, 2016, **424**, 37-44.
226 J. L. Lv, J. F. Zhang, J. Liu, Z. Li, K. Dai and C. H. Liang, *ACS Sustain. Chem. Eng.*, 2018, **6**, 696-706.
227 J. L. Liang, F. Y. Liu, J. Deng, M. Li and M. P. Tong, *Water Res.*, 2017, **123**, 632-641.
228 B. Yuan, C. H. Wang, Y. Qi, X. L. Song, K. Mu, P. Guo, L. T. Meng and H. M. Xi, *Colloids Surf. A Physicochem. Eng. Asp.*, 2013, **425**, 99-107.
229 J. S. Cai, J. Y. Huang and Y. K. Lai, *J. Mater. Chem. A*, 2017, **5**, 16412-16421.
230 W. J. Wang, S. J. Liang, K. N. Ding, J. H. Bi, J. C. Yu, P. K. Wong and L. Wu, *J. Mater. Sci.*, 2014, **49**, 1893-1902.
231 F. Ding, P. Chen, F. Liu, L. Chen, J.-K. Guo, S. Shen, Q. Zhang, L.-H. Meng, C.-T. Au and S.-F. Yin, *Appl. Surf. Sci.*, 2019, **490**, 102-108.
232 L.-N. Song, F. Ding, Y.-K. Yang, D. Ding, L. Chen, C.-T. Au and S.-F. Yin, *ACS Sustain. Chem. Eng.*, 2018, **6**, 17044-17050.
233 W. F. Zhang, J. W. Tang and J. H. Ye, *Chem Phys Lett*, 2006, **418**, 174-178.
234 W. F. Zhang, J. W. Tang and J. H. Ye, *J. Mater. Res.*, 2007, **22**, 1859-1871.
235 Y. P. Yuan, J. Lv, X. J. Jiang, Z. S. Li, T. Yu, Z. G. Zou and J. H. Ye, *Appl. Phys. Lett.*, 2007, **91**, 094107.
236 S. Moshtaghi, S. Gholamrezaei and M. S. Niasari, *J. Mol. Struct.*, 2017, **1134**, 511-519.
237 D. Chen and J. H. Ye, *Chem. Mater.*, 2007, **19**, 4585-4591.
238 T. Alammar, I. Hamm, V. Grasmik, M. Wark and A. V. Mudring, *Inorg. Chem.*, 2017, **56**, 6920-6932.

239 C. W. Lee, D. W. Kim, I. S. Cho, S. Park, S. S. Shin, S. W. Seo and K. S. Hong, *Int. J. Hydrogen Energy*, 2012, **37**, 10557-10563.
240 X. H. Zhang, J. D. Hu, Y. L. Cao, J. Xie, W. Jia, S. Q. Wang and D. Z. Jia, *Chem. Eur. J.*, 2018, **24**, 14111-14118.
241 X. H. Zhang, A. J. Liu, Y. L. Cao, J. Xie, W. Jia and D. Z. Jia, *New J. Chem.*, 2019, **43**, 10965-10972.
242 K. F. Moura, L. Chantelle, D. Rosendo, E. Longo and I. M. G. dos Santos, *Mater. Res-Ibero-Am. J.*, 2017, **20**, 317-324.
243 M. Kim, B. Lee, H. Ju, J. Y. Kim, J. Kim and S. W. Leek, *Adv. Mater.*, 2019, **31**, 1903316.
244 Y. P. Yuan, X. L. Zhang, L. F. Liu, X. J. Jiang, J. Lv, Z. S. Li and Z. G. Zou, *Int. J. Hydrogen Energy*, 2008, **33**, 5941-5946.
245 Y. P. Yuan, Z. Y. Zhao, J. Zheng, M. Yang, L. G. Qiu, Z. S. Li and Z. G. Zou, *J. Mater. Chem.*, 2010, **20**, 6772-6779.
246 T. Chen, J. Meng, Q. Y. Lin, X. Wei, J. X. Li and Z. Zhang, *J. Alloys Compd.*, 2019, **780**, 498-503.
247 J. Meng, Z. Y. Lan, Q. Y. Lin, T. Chen, X. Chen, X. Wei, Y. H. Lu, J. X. Li and Z. Zhang, *J. Mater. Sci.*, 2019, **54**, 1967-1976.
248 R. Borja-Urby, L. A. Diaz-Torres, P. Salas, E. Moctezuma, M. Vega and C. Angeles-Chavez, *Mater. Sci. Eng., B-Adv.*, 2011, **176**, 1382-1387.
249 J. Meng, X. Q. Fu, K. Du, X. Chen, Q. Y. Lin, X. Wei, J. X. Li and Z. Zhang, *Int. J. Hydrogen Energy*, 2018, **43**, 9224-9232.
250 A. S. Patra, M. S. Chauhan, S. Keene, G. Gogoi, K. A. Reddy, S. Ardo, D. L. V. K. Prasad and M. Qureshi, *J. Phys. Chem. C*, 2019, **123**, 233-249.
251 S. S. Fu, H. L. Niu, Z. Y. Tao, J. M. Song, C. J. Mao, S. Y. Zhang, C. L. Chen and D. Wang, *J. Alloys Compd.*, 2013, **576**, 5-12.
252 M. H. Wu, M. P. Luo, M. X. Guo and L. S. Jia, *ACS Sustain. Chem. Eng.*, 2017, **5**, 11558-11565.
253 L. Jia, J. Li and W. Fang, *J. Alloys Compd.*, 2010, **489**, L13-L16.
254 J. L. Xu, C. F. Sun, Z. Y. Wang, Y. D. Hou, Z. X. Ding and S. B. Wang, *Chem. Eur. J.*, 2018, **24**, 18512-18517.
255 C. Chen, J. L. Zhou, J. F. Geng, R. Y. Bao, Z. H. Wang, J. X. Xia and H. Li, *Appl. Surf. Sci.*, 2020, **503**, 144287.
256 J. Luo, J. Chen, R. Guo, Y. Qiu, W. Li, X. Zhou, X. Ning and L. Zhan, *Sep. Purif. Technol.*, 2019, **211**, 882-894.
257 T. K. Dhiman and S. Singh, *Phys. Status Solidi A*, 2019, **216**, 1900012.
258 C. D. Lv, G. Chen, J. X. Sun, Y. S. Zhou, S. Fan and C. M. Zhang, *Appl. Catal. B Environ.*, 2015, **179**, 54-60.
259 Y. Peng, K. K. Wang, T. Liu, J. Xu and B. Xu, *Appl. Catal. B Environ.*, 2017, **203**, 946-954.
260 K. Kamijyo, T. Takashima, M. Yoda, J. Osaki and H. Irie, *Chem. Commun.*, 2018, **54**, 7999-8002.
261 C. N. Ri, S. G. Kim, K. S. Ju, H. S. Ryo, C. H. Mun and U. H. Kim, *RSC Adv.*, 2018, **8**, 5433-5440.
262 T. T. Lv, D. Li, Y. Z. Hong, B. F. Lu, D. B. Xu, M. Chen and W. D. Shi, *Dalton Trans.*, 2017, **46**, 12675-12682.
263 M. J. Liang, Z. Y. Yang, Y. Mei, H. R. Zhou and S. J. Yang, *Nano*, 2018, **13**, 1850028.
264 C. D. Lv, G. Chen, J. X. Sun and Y. S. Zhou, *Inorg. Chem.*, 2016, **55**, 4782-4789.
265 F. Reyes-Pérez, J. J. Gallardo, T. Aguilar, R. Alcántara, C. Fernández-Lorenzo and J. Navas, *ChemistrySelect*, 2018, **3**, 10226-10235.
266 Z. Hong, W. K. Chong, A. Y. R. Ng, M. Li, R. Ganguly, T. C. Sum and H. S. Soo, *Angew. Chem. Int. Ed.*, 2019, **58**, 3456-3460.
267 D. X. Ju, X. P. Zheng, J. L. Liu, Y. Chen, J. Zhang, B. Q. Cao, H. Xiao, O. F. Mohammed, O. M. Bakr and X. T. Tao, *Angew. Chem., Int. Ed.*, 2018, **57**, 14868-14872.
268 W. Zhang, Q. Zhao, X. Wang, X. Yan, J. Xu and Z. Zeng, *Catal. Sci. Technol.*, 2017, **7**, 2753-2762.
269 X.-D. Wang, Y.-H. Huang, J.-F. Liao, Y. Jiang, L. Zhou, X.-Y. Zhang, H.-Y. Chen and D.-B. Kuang, *J. Am. Chem. Soc.*, 2019, **141**, 13434-13441.
270 Y. Guo, G. Liu, Z. Li, Y. Lou, J. Chen and Y. Zhao, *ACS Sustain. Chem. Eng.*, 2019, **7**, 15080-15085.

271 S. S. Bhosale, A. K. Kharade, E. Jokar, A. Fathi, S.-m. Chang and E. W.-G. Diau, *J. Am. Chem. Soc.*, 2019, **141**, 20434-20442.
272 G. Chen, P. Wang, Y. Wu, Q. Zhang, Q. Wu, Z. Wang, Z. Zheng, Y. Liu, Y. Dai and B. Huang, *Adv. Mater.*, 2020, **32**, 2001344.
273 B.-M. Bresolin, C. Günnemann, D. W. Bahnemann and M. Sillanpää, *Nanomaterials*, 2020, **10**, 763.
274 B.-M. Bresolin, P. Sgarbossa, D. W. Bahnemann and M. Sillanpää, *Sep. Purif. Technol.*, 2020, **251**, 117320.
275 B.-M. Bresolin, N. O. Balayeva, L. I. Granone, R. Dillert, D. W. Bahnemann and M. Sillanpää, *Sol. Energy Mater. Sol. Cells*, 2020, **204**, 110214.
276 Z.-L. Liu, R.-R. Liu, Y.-F. Mu, Y.-X. Feng, G.-X. Dong, M. Zhang and T.-B. Lu, *Solar RRL*, 2021, **5**, 2000691.
277 Y. Dai and H. Tüysüz, *ChemSusChem*, 2019, **12**, 2587-2592.
278 Y. Dai, C. Poidevin, C. Ochoa-Hernández, A. A. Auer and H. Tüysüz, *Angew. Chem. Int. Ed.*, 2020, **59**, 5788-5796.
279 L. Zhou, Y. F. Xu, B. X. Chen, D. B. Kuang and C. Y. Su, *Small*, 2018, **14**, 1703762.
280 Z. Zhang, Y. Liang, H. Huang, X. Liu, Q. Li, L. Chen and D. Xu, *Angew. Chem. Int. Ed.*, 2019, **58**, 7263-7267.
281 T. Wang, D. Yue, X. Li and Y. Zhao, *Appl. Catal. B Environ.*, 2020, **268**, 118399.
282 S. Kumar, I. Hassan, M. Regue, S. Gonzalez-Carrero, E. Rattner, M. A. Isaacs and S. Eslava, *J. Mater. Chem. A*, 2021, **9**, 12179-12187.
283 D. Wu, X. Zhao, Y. Huang, J. Lai, H. Li, J. Yang, C. Tian, P. He, Q. Huang and X. Tang, *Chem. Mater.*, 2021, **33**, 4971-4976.
284 Z. Zhang, Y. Yang, Y. Wang, L. Yang, Q. Li, L. Chen and D. Xu, *Angew. Chem. Int. Ed.*, 2020, **59**, 2005495.
285 Y. Hai, W. Huang, Z. Li, D. Wu, Q. Huang and X. Tang, *ACS Appl. Energy Mater.*, 2021, **4**, 5913-5917.
286 Y. Wu, Z. Gao, X. Sun, H. Cai and X. Wu, *Journal of Environmental Sciences*, 2021, **101**, 145-155.